Engineering Fracture Mechanics 257 (2021) 108036

Contents lists available at ScienceDirect

Engineering Fracture Mechanics

journal homepage: www.elsevier.com/locate/engfracmech

A state-of-the-art review of crack branching

Yanan Sun [a], Michael G. Edwards [a], Bin Chen [b], Chenfeng Li [a,c,*]

[a] Zienkiewicz Centre for Computational Engineering, College of Engineering, Swansea University Bay Campus, Swansea SA1 8EN, United Kingdom

[b] Lawrence Berkeley National Laboratory, Berkeley, CA 94720, United States

[c] Energy Safety Research Institute, College of Engineering, Swansea University Bay Campus, Swansea SA1 8EN, United Kingdom

ARTICLE INFO

Keywords:
Crack branching
Fracture propagation
Experiment
Criterion
Numerical simulation

ABSTRACT

Crack branching has important theoretical and practical significance in many natural phenomena and practical engineering problems. At present, the field of crack branching is still at an exploration stage, lacking a unified explanation of the underlying mechanisms and an effective method to predict crack branching in practical materials. This paper provides a state-of-the-art review of crack branching, including experimental observations, physics, fracture models and associated numerical methods. The experimental observations are first summarized, followed by the physics of crack branching. Then, the crack models including discrete crack models and smeared crack models are discussed, highlighting their key features, advantages and limitations. Next, a number of numerical methods that have been used to simulate crack branching are reviewed in detail, including the finite element method (FEM), extended finite element method (XFEM), boundary element method (BEM), meshfree methods (MMs), peridynamics (PD) and discrete element method (DEM). Finally, based on the information reviewed above, the future research directions of crack branching modelling are discussed.

1. Introduction

Crack branching is encountered in many practical engineering problems, and is particularly common in brittle materials and metal alloys with stress corrosion cracking [1,2]. As shown in Fig. 1, crack branching can occur symmetrically or asymmetrically. The study of crack branching phenomena, including branching mechanisms, branching criteria, experimental measurement and numerical simulation, is of great significance for robust and reliable prediction of crack propagation. A good understanding of the initiation and propagation of cracks inside structural materials is important for preventing catastrophic failure of engineering components and for developing new materials.

The theory of straight line crack expansion is basically mature, with the help of three main types of investigation techniques, namely experimental, analytical and numerical techniques. The mechanism for crack propagation is examined using the simple energy balance theory: the crack occurs when the energy available for crack growth is sufficient to overcome the resistance of the material [3]. In linear elastic fracture mechanics, the propagation criteria of a single steady crack are mainly based on the concept of stress intensity factor or energy release rate. While in nonlinear fracture mechanics, the J-integral is often applied, which can be viewed as a nonlinear stress intensity parameter or energy release rate. However, the mechanism for crack branching is more complex and still in exploration. The propagation velocity was thought to be a determining factor in crack branching: when the crack velocity exceeds the critical value, the stress field in front of the crack tip changes and branching occurs. However, it was later

* Corresponding author at: Zienkiewicz Centre for Computational Engineering, College of Engineering, Swansea University Bay Campus, Swansea SA1 8EN, United Kingdom.
E-mail address: c.f.li@swansea.ac.uk (C. Li).

https://doi.org/10.1016/j.engfracmech.2021.108036
Received 29 December 2020; Received in revised form 6 September 2021; Accepted 25 September 2021
Available online 2 October 2021
0013-7944/© 2021 Elsevier Ltd. All rights reserved.

Nomenclature

a_0 - a_7	Parameters in the Newmark method
A	Area
$\mathbf{b}$	Prescribed body-force density field
c	Peridynamic material parameter
c_d	Cohesion
c_R	Rayleigh wave speed
c_S	Shear wave speed
$E(\mathbf{u}, \Gamma)$	Energy functional
$E_\epsilon(\mathbf{u}, \Gamma)$	Regularized energy functional
$f(\phi)$	Energetic degradation function in phase field models
$\mathbf{f}$	Pairwise force in peridynamics
F_n, F_s	Normal force and shear force
F_{lm}	Dimensionless function of the branching angle coefficient when branching velocity tends to zero
$\{\mathbf{F}\}$	Global vector of nodal load
$g_1(v)$	Decreasing function of the crack velocity
G, G'	Energy release rate before and after branching
G^{dyn}	Dynamic energy release rate
G_c	Fracture toughness
$\mathcal{H}$	Horizon in peridynamics
H_{lm}	Dimensionless function of the branching angle coefficient and crack velocity before and after branching
$H(\mathbf{x})$	Heaviside function
$J(\mathbf{x})$	Junction function
$k(v), k_l(v')$	Function of crack velocity and branching velocity
k_n, k_s	Normal stiffness and shear stiffness
K_c	Initial stiffness in the intrinsic cohesive zone model
$K_I, {K_I}^{dyn}$	Stress intensity factor and dynamic stress intensity factor
${K_I}^0$	Instantaneous stress intensity factor
K_{Ib}	Critical branching stress intensity factor
K_{ID}	Dynamic crack growth toughness
K_l'	Dynamic stress intensity factor after branching
K_{0m}	Rest stress intensity factor before branching
$\mathbf{K}$	Stiffness matrix
l	Crack length
l_0	Length scale
$\mathbf{M}$	Mass matrix
N, N_c	Set of all nodes and cracked nodes
$\hat{N}_i, N_i$	Continuous shape function and discontinuous shape function
N^H, N^T, N^J	Set of nodes to enrich for the crack, the crack tip and the junction
$\mathbf{q}_i$	Additional degrees of freedom in cracking particles methods
r_c, r_0	Characteristic distance and instantaneous characteristic distance
s	Stretch of the bond
S	Sign function defined as 1 and −1 on two sides of the crack
t	Time
$\mathbf{t}$	Traction
$\mathbf{T}_c$	Cohesive traction
$\mathbf{T}_{ij}$	Fundamental solutions for traction
$\mathbf{T}_{max}$	Cohesive strength of the material
u_n	Normal displacement
$\mathbf{u}, \dot{\mathbf{u}}, \ddot{\mathbf{u}}$	Displacement vector, velocity vector, and acceleration vector

found that experimentally observed crack velocities at crack branches were much smaller than the theoretical ones [4]. Therefore, other mechanisms were considered, including the existence of microcracks, tilting and twisting of the stress vector at the crack front and dynamic instabilities. If near-tip instabilities are suppressed, then supersonic cracks are also possible [5]. While many studies

$\{\mathbf{u}\}, \{\dot{\mathbf{u}}\}, \{\ddot{\mathbf{u}}\}$	Global vectors of nodal displacement, nodal velocity and nodal acceleration
$[\![\mathbf{u}]\!]$	Displacement jump
$\mathbf{u}^h$	Displacement approximation
$\mathbf{U}_{ij}$	Fundamental solutions for displacement
v, v'	Crack velocity and branching velocity
v_c	Critical crack velocity
V	Volume of a material point
w	Crack opening
w_{max}	Maximum crack opening
$\mathbf{x}, \mathbf{x}'$	Position vectors of point $\mathbf{x}$ and $\mathbf{x}'$ in initial configuration
$\mathbf{X}$	Interior point in the boundary element method
$\mathbf{y}, \mathbf{y}'$	Position vectors of point $\mathbf{x}$ and $\mathbf{x}'$ in deformed configuration
$\boldsymbol{\alpha}_j, \boldsymbol{\alpha}_k^{\alpha}, \boldsymbol{\alpha}_m$	Nodal enriched degrees of freedom
β	Joint friction angle
γ, γ'	Fracture energy before and after branching
Γ	Crack set, or sharp crack surface
Γ_n^+, Γ_n^-	Upper and lower crack surfaces
Γ_S	The outer boundary
$\boldsymbol{\epsilon}(\mathbf{u})$	The strain field
λ	Branching angle coefficient
ρ	Mass density
ϕ	Damage-like crack phase-field parameter
$\boldsymbol{\Phi}_{\alpha}$	Near tip asymptotic field function
Ψ	Elastic energy density
Ω	A domain describing a cracked solid

on the crack branching phenomenon have been performed both experimentally and theoretically, a uniform theory that accounts for dynamic crack propagation instability and crack branching remains an open question.

In addition to the experimental and analytical techniques, numerical simulations are also employed to study crack branching. Various crack models and numerical methods have been proposed to simulate crack initiation and propagation including crack branching and intersection with reasonable computational cost, and both crack propagation velocity and branching angles have been correctly predicted. With the development of numerical techniques, the modelling of complex crack propagation processes has become more accurate and robust, while the mechanism of crack branching has been further understood. Crack models essentially divide into two categories: discrete crack models and smeared crack models. Popular discrete crack models usually represent the fracture topology explicitly, which include remeshing, element deletion, enrichment, cracking particles, and cohesive zone models. Smeared crack models average the crack over a certain width without explicit tracking of fracture surfaces, and they include nonlocal models, gradient models, viscous models and phase field models. Based on whether spatial derivatives are employed in the controlling equation, the main numerical methods for crack branching can also be summarized in two categories: continuum methods and discontinuum methods. The continuum methods model the domain as a continuous body and use partial differential equations with spatial derivatives to describe the underlying physics. They include the finite element method (FEM), the extended finite element method (XFEM), the boundary element method (BEM), and the meshfree methods (MMs). Spatial derivatives are avoided in the discontinuum methods. The peridynamic method (PD) and the discrete element method (DEM) are two commonly used discontinuum methods. Each numerical method has its advantages and disadvantages, and no consensus has been reached on a standard general numerical simulator for crack branching.

While dynamic crack propagation has been investigated in the literature [6,7], there has been little effort to systematically examine crack branching. Therefore, the aim of this work is to summarize the research on crack branching and lead to an improved understanding of branching mechanisms and the study direction in the future. The structure of the paper is arranged as follows. The experimental results on crack branching are summarized in Section 2. Based on the experimental results as well as the theoretical derivations, the physics of crack branching is provided in Section 3, which includes Section 3.1 describing the causes of crack branching and Section 3.2 describing commonly used branching criteria. Section 4 summarizes and compares different crack models and numerical methods for crack branching. Finally, Section 5 summarizes the existing findings related to crack branching, highlights some of the most demanding outstanding questions, and indicates potential directions for future research.

2. Experimental observations of crack branching

A number of experimental studies on dynamic crack propagation have been carried out to provide qualitative observations and quantitative data for the explanation of crack branching phenomena. In this section, the important experimental results are reviewed

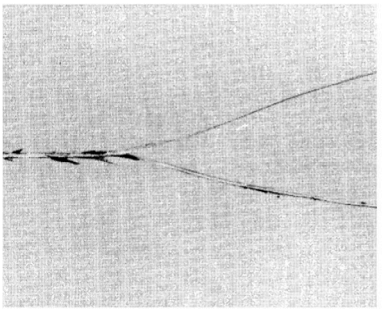

(a) Symmetrical crack branching [3].

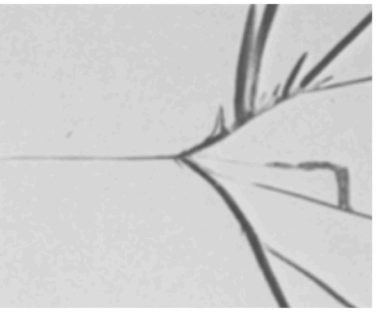

(b) Asymmetrical crack branching [4].

Fig. 1. Crack branching photographs from experimental results.

in chronological order and wherever applicable these experiments are summarized: (1) from the observation and measurement techniques, for example, the high speed photography and electronic timer; (2) from the experimental material, which includes inorganic glass, Plexiglas, Holmalite-100; (3) with respect to loading conditions such as dynamic loading and quasi-static loading; (4) from the research objectives, including the conditions under which crack branching occurs (crack tip speed, stress intensity factor and its rate) and how crack propagation proceeds after branching (e.g. the branching angle).

Schardin [8] performed pioneering work on observing crack branching in inorganic glasses with a multiple spark camera technique and noted that the crack speed remains at a constant value when crack bifurcation occurs. A significant decrease of crack speed only occurs when hackle marks appear as a result of surface energy increase. The number of crack branches greatly increases when increasing loading stress. Kerkhof [9] produced predictable crack surface undulation by imposing stress waves with ultrasonic transducers to measure the crack speed and proposed that the limiting velocity is highly related to the composition of inorganic glass. Kobayashi and Mall [10] and Dally [11] determined the dynamic fracture toughness of Homalite-100 and crack propagation velocity variation with dynamic photoelasticity. Dally [11] further modified the equation describing the relationship between the number of branches, the arrest toughness and branching toughness based on the experiment data. The number of branches is in proportion to the ratio of branching toughness to arrest toughness. Ravi-Chandar and Knauss [12,13,14,15] examined the dynamic crack propagation and branching problem in Homalite-100 comprehensively using high speed photomicrography with the load triggered by an electrical pulse. A series of important conclusions were obtained: (1) the stress intensity factor increases while crack velocity remains constant, and there exists a quantitative correlation between the stress intensity factor and the fracture surface roughness (mirror, mist and hackle); (2) from macroscopic examination of the fracture surface, it is found that a crack dissipates excess energy supplied to the crack tip by creating a rough surface rather than by changing the velocity of crack propagation; (3) from microscopic observations of fracture surface roughness, it is found that crack branching is a natural evolution from a "cloud" of microcracks that accompany and lead the main crack; (4) The terminal velocity in Homalite-100 was found to be $0.45c_R$, about half of the Rayleigh wave speed c_R.

Following the work by Ravi-Chandar and Knauss [12,13,14,15], Fineberg et al. [16,17],Sharon et al. [18],Sharon and Fineberg [19],Sharon et al. [20] investigated the micro-branch instabilities with a series of experiments performed on thin sheets of Plexiglas (PMMA). Fineberg et al. [16] designed an experimental system where the resistance voltage increases as a crack progresses across a sample and cuts the conductive layer, the crack velocity is measured by detecting the voltage. By plotting the evolution of crack velocity during crack growth, the existence of dynamic instabilities in a brittle fracture is detected. Fineberg et al. [17] found that once the crack velocity is greater than a critical value, dynamic instabilities occur and the amplitude of the oscillations depends linearly on the mean velocity of the crack. To explain the origin of instability, Sharon et al. [18] investigated the presence of microscopic local crack branching as a possible source for instability in dynamic fractures occurring in thin sheets of brittle PMMA. The crack micro-branches are observed and measured optically and a connection between microscopic and macroscopic crack branching is established. Later, with the same experiment system, Sharon et al. [20] measured both the energy flux into the tip of a moving crack and the total surface area created via the microbranching instability. It is found that a crack does not need to dissipate increasing amounts of energy by accelerating because it has another option of dissipating energy by creating an increased fracture surface, which provides an explanation for why the theoretical limiting velocity of a crack is never realized. Readers are referred to [21] for a comprehensive review of the early work on the micro-branching instability. In recent years, under the help of brittle poly-acrylamide gel (an aqueous elastomer), which enables probing the fracture process in unprecedented detail by high-speed cameras, a number of important experiments have been carried out to study the dynamic fracture process [22–25]. Fineberg and Bouchbinder [26] reviewed these experimental developments. It has been shown that (1) an intrinsic length scale, which is associated with nonlinear elastic deformation near the crack tip, plays an important role in dynamic instabilities; (2) dynamic instabilities include micro-branching instabilities and oscillatory instabilities. The micro-branching instability may be closely related to the oscillatory instability and it appears to be an intrinsically 3D instability instead of a 2D instability. Further discussions about the physics of crack branching can be found in Section 3.1.

A necessary and sufficient condition for crack branching was proposed by Ramulu and Kobayashi [4] (see further discussions in Section 3.2). Hawong et al. [27] verified the criteria by using the 16-spark-gap camera to record the dynamic photoelastic patterns

Table 1
Experimental techniques for crack branching.

Techniques		Advantages	Disadvantages
High speed photography	(Photoelasticity [10,11], caustics [37], holographic microscopy [29,38])	High temporal and spatial resolution	High cost
	(DIC [32], DGS [33])	High resolution, low cost, simple experimental setup	Low measurement accuracy in stress concentrations (DIC)
Wallner lines (stress wave fractography [39])		Accurate measurement for crack speed	low spatial resolution
Electrical resistance methods [30,40]		High spatial resolution	Sensitive to the variation of film thickness

of curving and branching cracks in Homalite-100 specimens under biaxial loading conditions. Increasing the biaxial stress ratio of horizontal loading to vertical loading and the stress level increases both the curvature and the number of branching cracks. Hauch and Marder [28] investigated the modes of energy dissipation in dynamic crack propagation and branching process in Homalite-100 by using a potential drop technique and made qualitative comparisons with PMMA. Suzuki et al. [29] investigated fast-growing cracks before and after bifurcation by using high-speed holographic microscopy and obtained the crack branching velocity, branching angles, and energy release rate in Homalite 100 and Araldite B. In Homalite 100 the crack branching velocity is $0.48C_R$ with an average branching angle of $17 \pm 6°$, and in Araldite B the crack branching velocity is $0.46C_R$ with an average branching angle of $16 \pm 4°$. The energy release rate increases gradually and continuously across the bifurcation point both in Homalite 100 and in Araldite B and PMMA. Murphy et al. [30] observed the branching patterns of PMMA single edge notched tensile specimens with scanning electron and optical microscopes and measured the crack propagation speed by electrical resistance methods. Each macroscopic branch is accompanied by many small cracks along its length with most crack branches being straight. The experimental results indicate that crack branching is a natural outcome of the growth and coalescence with microcracks. Both subsurface damage and the frequency of crack speed oscillations increase during the branching process. Fayyad and Lees [31] gave an example of using digital image correlation (DIC) to investigate the cracking process and branching mechanisms in lightly reinforced concrete beams. The DIC can visualize surface displacement by tracking the deformation of a random speckle pattern applied to the surface through digital images acquired at different instances of deformation [32]. Crack branching angles and propagation path are found to be related to the beam height and ductility. Another technique, called digital gradient sensing (DGS), employs 2D DIC with an elasto-optic effect to directly quantify both crack-tip fields and crack speeds. Using this technique, Sundaram and Tippur [33] investigated the branching phenomenon in soda-lime glass and proposed that the critical material length scale can be a criterion for crack branching. This study overcomes measurement challenges such as low fracture toughness and high crack propagation speed. Compared with normal observation and measurement techniques, the DIC and DGS have advantages of lower cost and simpler operation.

The advantages and disadvantages of different observation and measurement techniques are summarized in Table 1. In order to better explore the mechanism of crack propagation and branching, current research on experimental methods is focused on both the improvement of experimental technologies to overcome existing shortcomings and the development of new experimental technologies. With respect to testing materials, most experiments have adopted inorganic glass, Plexiglas, and Holmalite-100. The limiting velocity is studied in different materials and it is found that the limiting velocity is $0.5 \sim 0.65c_R$ for glass, $0.6 \sim 0.7c_R$ for PMMA and $0.35 \sim 0.45c_R$ for Homalite-100 [34]. The branching angles are also investigated although they are easily influenced by the loading conditions, geometry and material properties. From a macroscopic viewpoint, the angle subtended by the new branch (immediately after branching) and the original crack plane typically lies between 10° and 45° [35]. For different materials, detailed experimental results on branching angles can be found in [21,35,36]. The branch shape and branch number are also influenced by the loading conditions, geometry and material properties. The increasing of loading stress may lead to the increasing of branch number of the cracks while the loading conditions, geometry and material properties may have an impact on the branching angle as well as the branch curvature, thus, the branching shape.

3. Physics of crack branching

3.1. Causes of crack branching

Many attempts have been made to explain the crack branching phenomenon. One of the classical theories is from Yoffe [41]. On the assumption that the crack propagates along the direction normal to the maximum stress, when the velocity is lower than the critical velocity $0.6c_S$, where c_S is the shear wave speed, the crack propagation process remains at a steady state. When the crack velocity exceeds this critical value, the propagation process becomes unstable. The stress state at the crack tip will change, and the hoop stress in the vicinity of the crack tip will have a maximum angle of about 60° from the propagation direction, which may lead to crack branching, as shown in Fig. 2. By considering a crack growing from zero initial length at a uniform velocity rather than staying constant length, Broberg [42] further improved Yofee's analytical model and reaffirmed that crack branching occurs

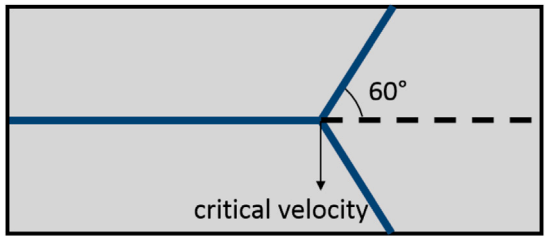

Fig. 2. Yoffe's crack branching model [41].

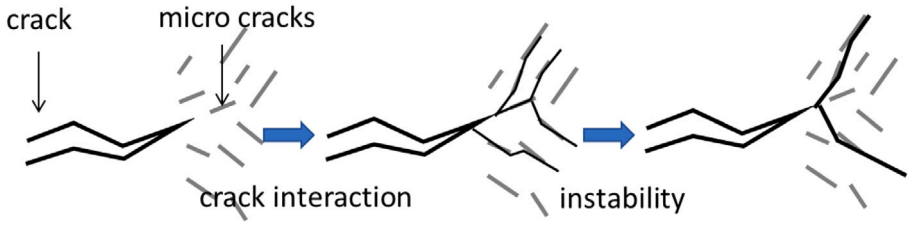

Fig. 3. Ravi-Chandar's micro crack model [14].

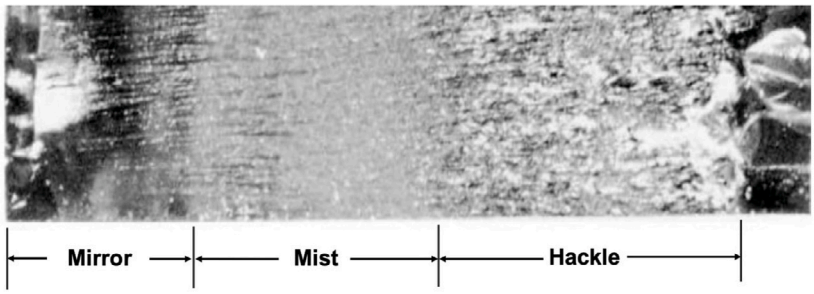

Fig. 4. Typical 'mirror', 'mist' and 'hackle' regions are identified in Homalite-100 [13].

if the velocity exceeds $0.6c_S$. The aforementioned studies suggest that the crack propagation become unstable and cracks are more likely to start branching when the velocity exceeds a critical value. This mechanism is corresponding to the "velocity criterion", see details in Section 3.2.1. Though this mechanism is not sufficient to explain the branching phenomenon, the velocity criterion resulted from it is often employed in numerical simulation due to its simplicity.

An alternate attempt to explain crack branching is via the viewpoint of energy. By assuming the energy inputting into the crack and the energy required to create new branch surfaces is balanced, Eshelby [43] argued that the crack tip velocity should at least be $0.5c_R$ to allow the energy at the crack tip to be sufficient enough to create new surfaces for crack branches, where c_R is the Rayleigh wave speed. However, according to the experimental observations, the crack velocity does not change significantly before and after crack branching [14]. Gao [44] explained that by proposing a more definitive analytic model called the wavy-crack model, where two velocities are defined: the macroscopic crack velocity v_a and the microscopic local velocity v_c. If the crack speed is above $0.5c_R$, the crack propagates along a wavy path and the energy absorbed into the crack is used to increase v_c while v_a remains constant. This explains why the crack speed does not decrease much after branching.

Another possible explanation is given by Ravi-Chandar and Knauss [14], who suggested that there exist many microcracks in front of the main crack as shown in Fig. 3, and branching is a natural outcome of the growth and coalescence of the microcracks. In Homalite-100, a varying fracture surface roughness during branching, 'mirror', 'mist', and 'hackle', can be observed [13], see Fig. 4. The fracture processes that occur over a spatial domain comparable to the surface roughness dominate the dynamics of crack growth. Initially, a crack propagates with a mirror-like fracture surface. Then, because of the coalescence of microvoids or preexisting defects ahead of the crack, the crack surface may become rough and subsequently microcracks form. The microcracks within the fracture process zone interact with each other and form micro-branches, which results in the final crack branching.

Following the work of [12–15], micro-branches and their instability have been studied in great detail recently by Fineberg et al. [17], Sharon et al. [18],Sharon and Fineberg [19],Sharon et al. [20], Fineberg and Marder [21], Bouchbinder et al. [22,23,24], Livne et al. [25], Fineberg and Bouchbinder [26], Livne et al. [45]. Using dynamic instabilities, these studies explain a number of long-standing problems in the dynamic fracture of amorphous including (1) velocity oscillations and limiting velocity, (2) fracture roughness, (3) the origin of the large increase in the energy dissipation of a crack with its velocity and (4) transition to crack

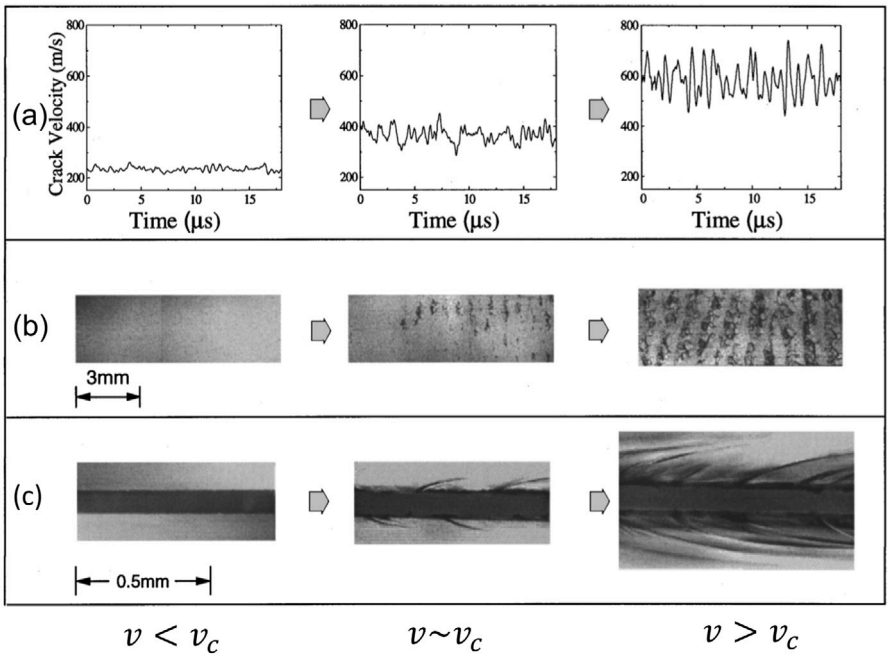

Fig. 5. Three aspects of the evolution of the branching instability as the crack propagates from left to right [19]. (a) The velocity of the crack is a smooth function of time when $v < v_c$, the crack velocity starts to oscillate when $v \sim v_c$, the oscillation amplitudes increase when $v > v_c$. (b) The fracture surface is smooth when $v < v_c$, small regions of different texture are distributed along the surface when $v \sim v_c$, these regions coalesce, forming a periodic pattern with wavelength on the order of 1 mm when $v > v_c$. (c) A single crack is observed when $v < v_c$, micro-branches appear when $v \sim v_c$, and increase in length when $v > v_c$.

branching. A detailed discussion about velocity oscillations and limiting is given in Section 3.2.1. When the crack velocity exceeds the critical value (limiting velocity), the velocity begins to oscillate rapidly [17]. A good correlation is demonstrated between the measured crack velocity and appearance of fracture roughness on the fracture surface [19], see Fig. 5. The initial crack with a velocity lower than the critical crack velocity v_c corresponds to a mirror-like fracture surface. After achieving the critical crack velocity v_c, the velocity begins to oscillate. As the velocity increases, rib-like patterns observed on the fracture surface become more apparent. Microscopic branches have also been observed when the velocity exceeds the critical value. These characteristic features are independent of the brittle material due to the fact that in two extremely different classes of material (poly-acrylamide gel and soda-lime glass), identical characteristic behaviour is observed [45]. The origin of the large increase in the energy dissipation of a crack with its velocity can also be explained by the micro-branching instability [20]. When micro-branching instabilities occur, the energy dissipation of a crack increases because more surfaces are formed by the micro-branches. As the velocity of the crack increases, transition to crack branching occurs with the branches becoming longer and more numerous. Micro-branches can smoothly transform to macro-branches with similar characteristic features of crack branching exhibited between the micro-branches and macro-branches [18]. The onset of the micro-branching instability therefore provides a well-defined criterion for the process that eventually culminates in macroscopic crack branching. As the crack velocity increases larger than the critical velocity, the branch width increases and the surface roughness diverges. This transition may be a sufficient condition for macroscopic crack branching to occur [19]. The dynamic instabilities have been further studied with a series of theoretical work [22–24] and with experiments in brittle gels [25]. A weakly nonlinear theory of dynamic fracture has been introduced, which implies that the understanding of crack instabilities requires the introduction of new physical ingredients, e.g. length scales [24]. Intrinsic nonlinear scales in the near-tip region play a decisive role in dynamic crack instabilities. Fineberg and Bouchbinder [26] gave a comprehensive review of important experimental and theoretical work in dynamic crack instabilities, which states that the micro-branching instability is an intrinsically 3D instability and to understand the dynamic instabilities, the framework of fracture mechanics should be extended to include 3D crack propagation.

Through theoretical analyses, Adda-Bedia and Arias [46],Adda-Bedia [47,48], Katzav et al. [49], Adda-Bedia et al. [50] systematically studied the crack branching mechanisms including dynamic crack instability and 3D microbranching instability. Based on the theory of linear elastic fracture mechanics and Eshelby [43]'s energy approach which states that the energy input into a crack and the energy required to create new branch surfaces must be balanced, the theoretical model for branching instabilities was established [46]. Dynamic crack branching instability under general antiplane loading [47] and under general loading [48] are studied and the path and geometry of the branched crack are predicted. It is shown that after branching the in-plane elastic fields immediately exhibit self-similar properties, and the jump in the energy release rate is maximized. Under this assumption, the crack branching phenomenon, which is found to be energetically possible, may be seen as a dynamic instability in which a self-similar

single crack propagation would lose its stability at some point dependent on crack velocity [49]. Later, Adda-Bedia et al. [50] investigated the 3D out-of-plane nature of crack front waves (generated by both the interaction of a crack with a localized material inhomogeneity and the intrinsic formation of micro-branches [51]) and the microbranching instability with the Willis–Movchan 3D linear perturbation formalism. It is demonstrated that within a minimal linear elastic fracture mechanics scenario, the existence of an out-of-plane crack front instability is dependent on critical velocity, which may trigger a 3D microbranching instability and its fractographic implications.

For materials like inorganic glasses, where microcracks cannot be found in front of the main crack, different mechanisms have been proposed. Hull [39] suggested micro-scale variations lead to twisting and tilting of the stress vector near the crack tip, cause local instability to the dynamic properties of cracks, and are responsible for the increase of crack surface roughness and crack branching. Sharon et al. [51], Bonamy and Ravi-Chandar [52] tried to explain the surface roughening from the interaction of the shear wave with the tip of the growing crack. The shear wave proves the existence of front waves in dynamic fractures. The front waves feature an out-of-plane component, which leaves marks on the fracture surfaces and causes surface roughness and crack shape perturbations [26].

Though crack branching in dynamic fractures has long been observed and investigated in various literatures, up to now, there has not been a universally agreed-on explanation for crack branching mechanisms. Based on the above work, the mechanisms of branching can be summarized as: (1) the increase of the velocity may cause unstable crack propagation, which causes crack branching; (2) the microvoids and microcracks may increase surface roughness and the growth and coalescence of microcracks which form micro-branches resulting in macro-branches with the energy absorbed in the crack relating to the limiting velocity; (3) the dynamic instability plays an important role. Cracks undergo an oscillatory instability controlled by small-scale, near crack-tip, elastic nonlinearity, and this oscillatory instability may trigger microbranching instability, which provides a well-defined criterion for the process that eventually culminates in macroscopic crack branching; (4) the crack front waves and the tilting and twisting of the stress vector at the crack front may cause local dynamic instability, increasing of crack surface roughness leading to crack branching.

3.2. Branching criteria

Crack branching criteria tend to be artificially formulated based on physical mechanisms to improve crack branching simulation. We divide the criteria into two types: external criteria and internal criteria. Here, "external" means that in the numerical simulation additional criteria are needed to determine how the crack branching occurs. The criteria required in a whole process for branching simulation include criteria for crack initiation, criteria for crack propagation, criteria for crack branching time and criteria for branching angles. A series of studies on criteria for dynamic crack initiation and crack propagation are summarized in dynamic fracture mechanics [6,7]. The following discussion will focus on criteria for branching time and branching angles, instead of being exhaustive. In contrast to the "external", "internal" means that no additional criteria are required, and any occurrence of branching is a natural outcome of the simulation.

3.2.1. External criteria

To determine the branching time, three commonly used criteria are introduced, namely the velocity criterion, the stress intensity factor criterion, and the energy criterion.

Velocity criterion. The velocity criterion suggests that once the crack velocity exceeds a critical value, branching occurs. Note that there exists two branch types, namely micro-branches and macro-branches, which are discussed separately here. Both theoretical and experimental approaches have been used to investigate the critical velocity of a fast moving crack.

An energy balance equation was given by Freund [6], which considers a crack growing with a nonuniform speed under time-independent/dependent loading:

$$G^{dyn} \approx (1 - \frac{v}{c_R}) {K_I}^0(t, l(t), 0) = \gamma \tag{1}$$

where G^{dyn} is the dynamic energy release rate, v the crack velocity, ${K_I}^0(t, l(t), 0)$ the instantaneous stress intensity factor at time t for a stationary crack of length $l(t)$ and γ the fracture energy. Based on Eq. (1), the fracture energy for a moving crack will vanish when the crack velocity v increases to the Rayleigh wave speed c_R. Therefore, from the elastodynamic fracture mechanics theory, the limiting velocity for crack propagation is no larger than the Rayleigh wave speed. However, from an experimental view, it is found that only cracks on the cleavage planes in crystalline materials grow at a rate close to Rayleigh wave velocity. For cracks in noncrystalline materials, the limiting velocity of the crack is significantly smaller than the theoretically predicted limiting crack velocity [7]. The reason behind this phenomenon can be explained by dynamic instabilities [17]. Indirect evidence to support this is that when the dynamic instability is suppressed, the crack may propagate at a supersonic speed [5]. Mechanisms behind the supersonic crack propagation problems are explored by Buehler et al. [53], Abraham and Gao [54].

The critical velocity for micro-branches states that once the velocity exceeds the critical velocity v_c, crack propagation becomes unstable with the occurrence of velocity oscillations, and the increase of surface roughening and microbranching [21]. The critical velocity for instability and micro-branches has been investigated with experimental approaches. Fineberg et al. [16,17] made detailed measurements indicating that the critical velocity for crack propagation in PMMA is $0.36c_R$. Hauch and Marder [28] and Ravi-Chandar and Knauss [13] observed the critical velocity for crack propagation in Homalite is $0.37c_R$. Gross et al. [55] showed the critical velocity for crack propagation is $0.42c_R$ in soda-lime glass. Based on the experimental observations above, the

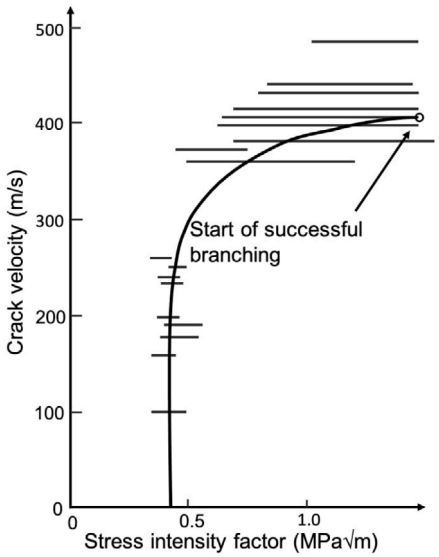

Fig. 6. Relationship between crack velocity and stress intensity factor in (brittle) Homalite 100 (solid curve). The "horizontal" lines represent measurements of the tip motion of cracks in large plates as they grow with no or minimal influence of stress waves reflected from the plate boundaries, adopted from [11].

existence of a critical velocity for the instability of brittle fracture may be a universal aspect [17]. Though the micro-branches instability is seen as one of the reasons for crack branching, the transition from critical velocity criterion for micro-branches to critical velocity criterion for macro-branches is still unknown [21]. The critical velocity for macro-branches is used to determine when macro-branches develop. Theoretically, as discussed in Section 3.1, various authors established models to analyse the critical velocity. The critical velocity is assumed to be $0.6c_S$ in Yoffe [41]'s model, $0.5c_R$ in Eshelby [43] and Gao [44]'s model, $0.52c_R$ in Adda-Bedia [48]'s model. Experimentally, as discussed in Section 2, the limiting velocity is $0.5 \sim 0.65c_R$ for glass, $0.6 \sim 0.7c_R$ for PMMA and $0.35 \sim 0.45c_R$ for Homalite-100.

In addition, many experimental results show that the crack velocity does not change significantly after branching [14]. These limitations have challenged or weakened the velocity criterion for crack branching. However, due to its simplicity, the velocity criterion is widely used in numerical simulation for crack branching. For example, Linder and Armero [56] proposed a branching model using FEM, where branched elements are added to represent discontinuities if the crack velocity exceeds a given threshold. The influence of different critical velocities on branching was investigated with the FEM-based model. Using a similar model, Armero and Linder [57] successfully captured the crack propagation path and branching characteristics. Xu et al. [58] set up the additional enrichment in XFEM to describe crack branching and adopted the branching time criterion from Yoffe [41], where the crack branching occurs when the maximum normalized circumferential stress occurs in two symmetrical directions. The critical velocity during simulation is found to be over $0.74c_R$. By comparing the numerical result $0.74c_R$ with the experimental result $0.4c_R$, they concluded that the crack velocity error was due to the velocity criterion adopted.

Stress intensity factor (SIF). In elastodynamic fracture mechanics, the theoretical framework is fairly well established through a series of studies of a dynamically propagating crack in an infinite body by Freund [6,59,60,61]. Taking mode I crack as an example, the dynamic crack growth criterion is given as:

$$K_I^{dyn}(t, v) = K_{ID} \tag{2}$$

where K_I^{dyn} is the dynamic SIF, t the time, and K_{ID} the dynamic crack growth toughness. For the left-hand side of the Eq. (2), theoretically, the dynamic SIF is related to both the crack velocity and the instantaneous SIF of a stationary crack, which can be expressed as:

$$K_I^{dyn}(t, v) = k(v)K_I^0(t, l) \tag{3}$$

where $k(v)$ is a function of crack velocity and K_I^0 is the instantaneous SIF of a stationary crack with length l at time t. Numerically, the dynamic SIF can be calculated through J-integral or interaction integral. Unlike the calculation in quasi-static conditions, the numerical calculation of J-integral or interaction integral is no longer path independent in dynamics. The reader is referred to the book by Anderson [3] for more details. For the right-hand side of Eq. (2), the crack growth toughness K_{ID} can be determined experimentally, and the K–v relationship is often employed. Experimentally, the dynamic SIF is related to crack velocity, however, the relationship is not unique, but an average can be obtained [7,11], see Fig. 6.

By experimental investigations, Kobayashi and Mall [10] and Dally [11] indicated that branching occurs when the SIF reaches a critical value that is between two and three times the quasi-static fracture toughness of the material. Clark and Irwin [62] suggested

that the dynamic SIF should reach a critical value for branching to occur at terminal velocity. Based on previous theoretical and experimental studies on crack curving and crack branching, Ramulu and Kobayashi [4] proposed the following necessary and sufficient conditions for crack branching:

$$\begin{aligned} &K_I \geq K_{Ib} \rightarrow \text{necessary condition} \\ &r_0 \leq r_c \rightarrow \text{sufficient condition} \end{aligned} \tag{4}$$

where K_{Ib} is the critical branching SIF, and r_c is the characteristic distance from the crack tip. With experimental observations, Ravi-Chandar [7] concluded that a crack will split into two or more branches if it reaches the critical stage identified by its SIF, and each branch will propagate with the same speed as the parent crack. The SIF criterion is applied to decide crack branching time when modelling crack propagation [63,64]. Kishen and Singh [63] simulated crack development (crack kinking and branching) on the rock-concrete interface of a gravity dam using the SIF-based fracture criterion. Using a time-domain BEM approach, Rafiee et al. [64] examined dynamic crack propagation, where a critical mode I SIF was used for the branching event and the maximum circumferential stress criterion was employed for determining the branching angle and each branch's growth rate.

Energy criterion. The energy criterion is applicable to both linear and nonlinear fracture mechanics, e.g. the energy release rate G and the J-integral. The crack extension occurs when the energy available for crack growth is sufficient to overcome the resistance of the material [65].

Eshelby [43] proposed the branching criterion theory based on the balance between the energy inputting into the crack and the energy required to create new branch surfaces. Based on this study, with the help of the Griffith's energy criterion and the principle of local symmetry, Adda-Bedia [47,48] presented a series of analytical solutions for crack branching problems. The energy criterion was assumed to be a necessary condition for a branching configuration, and the stress field in front of the crack tip, the branched shape and the dynamic branching instability were predicted and analysed. Tchouikov et al. [66] calculated the energy flux per unit time into the crack tip with a dynamic J-integral. Once a given critical energy release rate is surpassed, the branch occurs and an implicit prediction for branching path is adopted. Xie et al. [67] derived an energy-based fracture mode for the mode-I crack branching, where branching toughness was proposed, the branching critical energy release rate was derived and the branching angle was predicted. The criterion shows good agreement with the experimental observations reported in the literature.

Criteria for branching angles. After the branching time is determined, the next step is to determine how the crack propagates with branching. The branching angle has been studied both experimentally and theoretically. Experimentally, as discussed in Section 2, the angle subtended by the new branch (immediately after branching) and the original crack plane typically lies between 10° and 45°. Theoretically, the crack propagation direction can be predicted by the maximum circumferential stress theory, the minimum strain energy density factor theory, the principle of local symmetry and the maximum strain energy release rate theory [4]. A comprehensive review of earlier analytical research work on elastostatic and elastodynamic self-similar crack branching problems in homogeneous, isotropic and elastic brittle solids was given by Dempsey [35]. The number of elastodynamic solutions is quite limited compared with the number of elastostatic solutions. For planar elastodynamic crack propagation, Yoffe [41] attempted to explain the branching of cracks by analysing a problem in which a crack of constant length moving along a straight line with a uniform speed in an infinite two-dimensional medium. It is found that the maximum stress moves out of the plane of crack propagation and acts at an angle of 60° to the main crack propagation direction when the velocity is lower than the critical velocity $0.6c_S$. For elastodynamic crack propagation under antiplane loading, Dempsey et al. [68], Burgers [69,70] derived analytical solutions for a semi-infinite crack that starts to propagate from rest by kinking or branching under the action of a stress pulse loading.

To obtain a more general solution for the dynamical crack kinking or branching problem, a series of studies were conducted by Adda-Bedia and Arias [46],Adda-Bedia [47,48]. To predict the crack path, the determination of the elastodynamic fields associated with kinked or branched cracks is required. Adda-Bedia and Arias [46] presented a new method to determine the elastodynamic stress field/the dynamic SIF associated with the propagation of anti-plane kinked or branched cracks. The theory was applied to the case of dynamic crack branching under general antiplane loading [47] and later the general antiplane loading condition was extended to arbitrary loading condition [48]. The SIF just after branching was given as a function of the SIF just before branching, the branching angle and the branching velocity [48]:

$$K_l' = \sum_m k_l(v') H_{lm}(\lambda, v, v') K_{0m} \tag{5}$$

where K_l' and K_{0m} are the dynamic SIF just after branching and the rest SIF just before branching, respectively, l and m =1, 2, 3, $k_l(v')$ is a universal function of the branching velocity v', and H_{lm} is a dimensionless function of the branching angle coefficient λ, and of the crack velocity before and after branching. When $v' \rightarrow 0$, it can be expressed as:

$$H_{lm}(\lambda, v, v' \rightarrow 0) = F_{lm}(\lambda) \tag{6}$$

Taking Mode I crack as an example, to get the branching angle, the Griffith energy criterion and the principle of local symmetry are employed. The Griffith energy criterion states that the energy release rate G during crack propagation is equal to the dynamic fracture energy γ of the material [71]. For crack branching, the relationship between the energy release rate G, fracture energy γ before branching and the energy release rate G', fracture energy Γ' after branching can be obtained:

$$G' = G\frac{\gamma(v')}{\gamma(v)} \tag{7}$$

According to the principle of local symmetry, which states that the crack always propagates in a direction that the local stress field at the crack tip is of mode I type [72], the following conditions are satisfied immediately after branching:

$$g_1(v) = F_{11}^2(\lambda) \tag{8}$$

$$F_{21}(\lambda) = 0 \tag{9}$$

where $g_1(v)$ is a decreasing function of the crack velocity v with $g_1(0) = 1$ and $g_1(c_R) = 0$. By solving the equations above, a critical velocity for branching and a branching angle can be obtained. When the velocity exceeds a critical value of $0.52c_R$, a crack starts to branch at a branching angle $\lambda\pi = 27°$ corresponding to $\lambda = 0.15$. The predicted result agrees well with the available experimental results [17,21]. Detailed analytical solutions for other loading modes were given by Adda-Bedia [48]. Based on the above work, Katzav et al. [49] further summarized the theory of dynamic crack branching in brittle materials. With the theory, a systematic analysis of the branching problem is made, and the critical velocity, the branching angle, the branching velocity, and the subsequent branch path described by a curvature parameter are successfully predicted.

3.2.2. Internal criteria

Internal criteria are combined with numerical methods and embedded in the specific crack models, which leads to crack branching as a natural outcome of the simulation. A simple way to judge whether a model or a method contains internal criteria is to check whether branching angle criteria are required during simulation. If not, cracks are allowed to form freely in the simulation. Models and methods containing internal branching criteria include, but are not limited to, the cracking particles method, the peridynamics, the phase field model, the element deletion model, the cohesive zone model, the enrichment models and nonlocal models/gradient models/viscous models. Among them, the cohesive zone model, the cracking particles method, the phase field model, and the peridynamics, which are representative, are briefly introduced in this section, while more detailed information about all these models and methods can be found in Section 4.

In the cohesive zone model, the traction–separation law defines the relationship between the crack width (distance between the crack surfaces) and the cohesive traction in the process zone. The crack surfaces begin to separate when the cohesive strength is reached, and when the separation reaches a critical value, the traction decreases to zero and failure occurs. Crack branching naturally forms in the solution of the initial–boundary value problem without any branching criteria [73,74]. In the cracking particles method, the crack is described by the set of cracked particles [75–77]. A cracking criterion is employed to crack the particle and create a discrete crack. The crack is modelled by a set of discrete cracks. During simulation, no external criteria are required to determine the branching time and branching angles, and the crack develops by breaking particles in a sequence. In the peridynamics, the material can be considered as a collection of points [78]. If as a result of various forces, two points of the material are separated by a distance beyond a critical value, the interaction (bond) between the two points will vanish (break). Only one critical value for a bond break is needed. Once the stretch exceeds the critical value, failure starts to occur and under certain boundary conditions, crack branching is observed without additional criteria for branching [78]. The phase field model is developed in the form of a variational theory of fractures based on the principle of minimum total potential energy. Through defining the total potential energy of a material body with cracks, it turns the crack propagation problem into an energy minimization problem. By giving boundary conditions, the unknown displacements and the crack path can be solved via global minimization. Thus, in theory, there is no need of external branching criteria, and the only rule required for crack initiation or propagation is that: compared to the previous configuration, the new configuration leads to the lower total energy. Similarly, crack branching is allowed if lower potential energy can be obtained than a simple extension.

4. Crack models and numerical methods

Crack models are used to describe how to represent the fracture, including the geometry and the stress concentration. Numerical methods are employed to solve equations, describe the bulk material behaviour, and capture the fracture propagation process. Different models can be combined with each other and they can be integrated with multiple numerical methods. Likewise, different numerical methods can be combined to form hybrid methods, and they can also work with different fracture models, see Fig. 7. Smear crack models can account for the crack tip nonlinearity. While discrete fracture models integrated with notable methods such as finite element method, extended finite element method, boundary element method often do not account for crack tip nonlinearity unless the cohesive zone model is employed.

4.1. Crack models

Crack models are used to describe how to represent the crack, and they can be roughly divided into two categories: discrete crack models and smeared crack models. Based on how the crack is represented, the "discrete" means the crack topology is explicitly represented while the "smeared" means the crack is smeared over a certain width without explicit tracking of crack surfaces. Popular discrete crack models include remeshing, element deletion, cracking particles, and enrichment models. Popular smeared crack models include phase field, nonlocal, gradient and viscous models. Note that different from the models mentioned above which describe how to represent cracks, the cohesive zone model describes the nonlinear behaviour in the process zone ahead of the crack tip with a traction–separation law and it is essentially a discrete concept. Therefore, we describe the cohesive zone model as part of the discrete crack models. However, it can also be implemented in smeared context by distributing the work of separation or fracture energy over the width of an element [79]. See [80] for various smeared representations of cohesive-zone type behaviour. As a summary, Table 2 lists the advantages and limitations of different crack models, and their details are separately discussed in the following subsections.

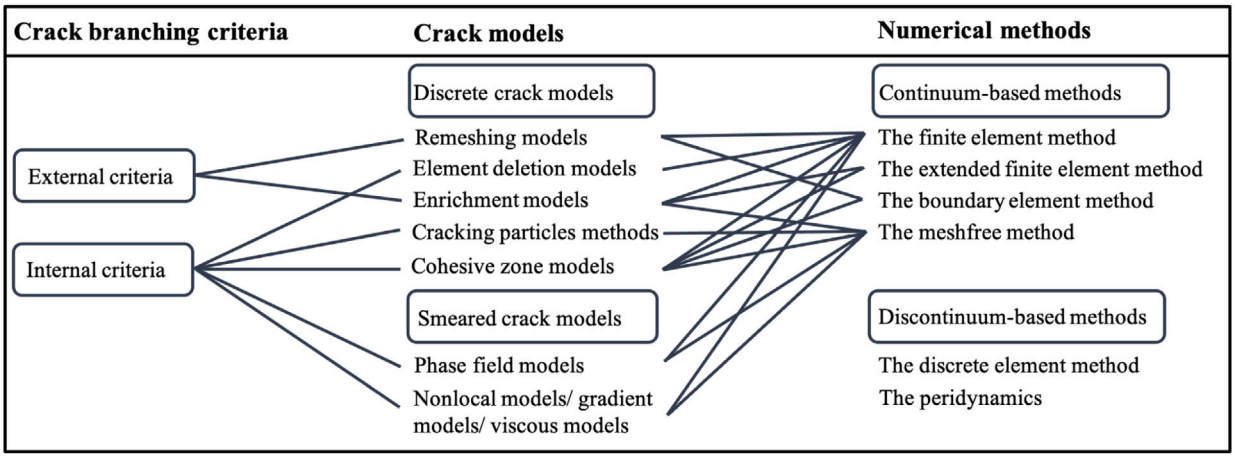

Fig. 7. Crack models and numerical methods.

Table 2
Advantages and limitations of different crack models for crack branching.

Crack Models	Advantages	Limitations
Remeshing models [2,66]	Flexible in dealing with complex geometries and boundary conditions	Awkward in dealing with complex three-dimensional geometries
Element deletion models [81–83]	Easy implementation	special treatment is required to solve the mesh dependency
Enrichment models [84–86]	Solve parts of difficulties associated with the mesh	Rely on different types of enrichment adopted, see more detail in Section 4.2
Cracking particles methods [75–77]	Suitable for complex crack patterns, straightforward implementation in 3D	Special treatment is required to solve the "spurious cracking" problems and reduce the computational cost
Cohesive zone models [73,74]	Suitable for complex crack patterns, removes singularity in the crack tip	Special treatment is required to solve the mesh dependency and bias
Phase field models [87,88]	Suitable for complex crack patterns, straightforward implementation in 3D	Fine mesh is required to obtain more accurate results
Nonlocal models/gradient models/viscous models [89,90]	Solve the ill-posed boundary value problem, suitable for modelling failure caused by progressive damage	Physical inconsistencies may appear, fine mesh is required to obtain more accurate results

4.1.1. Discrete crack models

Remeshing models. As the crack propagates and branches, new discontinuities form across the crack, therefore, crack surfaces need to be redefined as boundaries and the mesh needs to be updated. Remeshing models update the crack surface with remeshing techniques, where an explicit representation of crack surfaces and a crack tracking algorithm are usually required. During the simulation process, external criteria including the crack initiation, propagation, branching time and angle criterion are employed, which increases the difficulty of computational simulation. The reasons are manifold: (1) until now, there is no universally agreed explanation for branching time and branching angles; (2) the formula to calculate the associated parameters under dynamic situation remains a challenge; (3) a remeshing rule including the selection of element type, mesh generation method, data transfer during remeshing is required for which computation efficiency needs to be considered.

The remeshing models can be combined with such numerical methods as FEM and BEM to simulate crack branching. A schematic illustration of crack branching with remeshing models based on FEM is shown in Fig. 8. Compared with remeshing models based on FEM, remeshing models based on BEM is much simpler due to the reduced dimensional features of BEM. Details will be explained in Section 4.2. Both methods assume that the crack surface is generally determined by the separation between elements, which makes it difficult to capture crack surface roughness relating to dynamic brittle fracture. Note that another commonly used application of the remeshing models is its combination with cohesive zone models by actively inserting cohesive interface elements into the finite element mesh, which will be discussed separately later.

Element deletion models. Element deletion models are often integrated with FEM, where the crack is represented by a set of deleted/deactivated elements, as shown in Fig. 9. There is no need for explicit representation of the crack's topology by remeshing. The deactivation of elements can be achieved through two approaches: (1) complete element deletion technique, in which deleted elements are replaced by rigid masses and (2) setting the stress of the deactivated elements to zero [81,91]. The elements, which are deactivated or deleted, have no material resistance or stress for the rest of the simulation process [92].

However, unless the constitutive equation is properly scaled or adjusted, the released energy due to deleting an element will depend on the element size, which can cause spurious mesh dependency and lead to high computational cost in dynamic crack

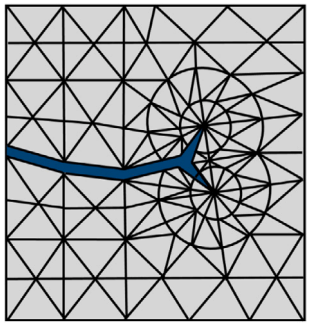

Fig. 8. A schematic illustration of crack branching with remeshing models based on FEM.

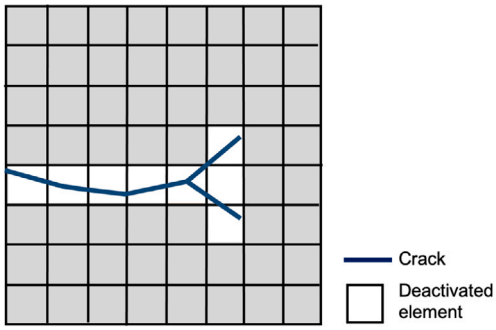

Fig. 9. A schematic illustration of crack branching with element deletion models.

simulations [93]. To reduce the spurious mesh dependency, the softening curve slope should be scaled so that fracture energy is independent of the element size [81]. The mesh dependency problem is also handled with variational formulations [82]. Schmidt et al. [94] proposed a promising approximation scheme named "eigenfracture", in which the deformation is seen as an eigen-deformation in the eroded element and a nonlocal regularized fracture energy is introduced to eliminate the mesh dependence. Derived from the eigenfracture, Pandolfi and Ortiz [82] developed a method called "eigenerosion", which is characterized by the restriction of element erosion in a binary sense: it can be equal to 0 if the element is eroded or 1 in case of fully elastic behaviour. The fracture propagation is then treated as failing elements when the elastic energy release is higher than the corresponding dissipated fracture energy. Compared with the original element deletion model, the eigenerosion, as an extension version, is more suitable for crack branching problems for its accuracy and convergence in complex crack simulations [81–83,94].

Song et al. [81] checked the performance of the element deletion model for dynamic crack propagation in brittle materials and found that the element deletion model gives a very irregular crack velocity and performs poorly for the accurate prediction of crack branching. Based on the eigenerosion, Stochino et al. [83] introduced a modified formulation of eigenfracture, where the compression and tension loaded state is distinguished. The efficacy of the approach is proved by a dynamic crack branching example. It is found that the crack branching time depends on the fracture resistance of the structure related to the critical energy release rate and numerical parameter settings. To reduce the high computational cost caused by a relatively fine mesh during modelling, Fan et al. [95] presented a dynamic adaptive eigenfracture scheme by combining the eigenfracture scheme and the adaptive mesh refinement algorithm, which reduces the element size locally while improving the Griffith fracture convergence property. The ability of the dynamic adaptive eigenfracture scheme in predicting crack propagation was proved by numerical examples of crack branching, see Fig. 10. It is found that the crack pattern, the crack branching velocity and crack instabilities in the simulation are in good agreement with the experimental observations.

The element deletion model deletes elements that satisfy a certain criterion explicitly and no additional criteria are required to determine the branching time and branching angles. However, special treatment is required to solve the mesh dependency problem [93]. The mesh needs to be fine enough to obtain accurate crack path prediction in dynamic crack simulations, which may in turn cause high computational cost. To the best of the author's knowledge, till now, the number of studies on the performance of the element deletion model in dynamic crack branching simulation is limited [81,83,95], and no 3D examples are provided. Though its ability in modelling the crack pattern and the crack branching velocity has been proved in 2D [95], more investigations such as multiple crack branches, crack branching in 3D are yet to be demonstrated.

Enrichment models. The enrichment models use the so-called "enrichment approaches" to account for the discontinuous displacement fields in the crack. The enrichment approach is to enrich a polynomial approximation space so that the crack can be modelled independently of the mesh. There are commonly two types of enrichment, namely, the intrinsic enrichment and the extrinsic

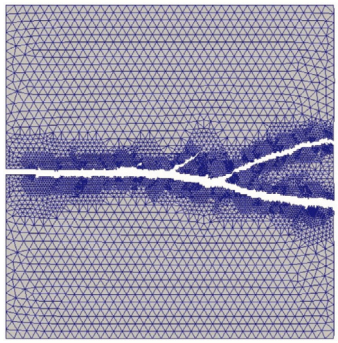

Fig. 10. A numerical example of crack branching with element deletion models [95].

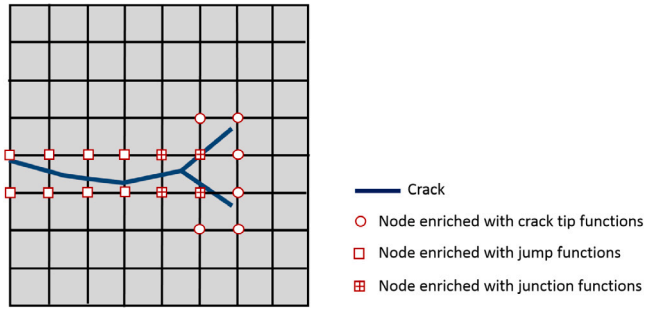

Fig. 11. A schematic illustration of crack branching with enrichment models combined with XFEM.

enrichment. The intrinsic enrichment is to replace (at least some of) the shape functions in the polynomial approximation space with special shape functions. The number of shape functions and unknowns is unchanged during simulation. While the extrinsic enrichment can be achieved by adding special shape functions to the polynomial approximation space, where more shape functions and unknowns result in the approximation [96].

The enrichment model can be combined with XFEM or MMs. Fries and Belytschko [96] summarized important features about enrichment in XFEM: (1) the enrichment is extrinsic and realized by the partition of unity (PU) concept; (2) the enrichment is local because only a subset of the nodes is enriched; (3) the enrichment is mesh-based, i.e. the PU is constructed using standard FE shape functions; (4) enrichments for arbitrary discontinuities in the function and their gradients are available. A schematic illustration of crack branching with enrichment models combined with XFEM is shown in Fig. 11. Compared with the enrichment in XFEM, the enrichment in MMs can be both intrinsic and extrinsic. The extrinsic enrichment can be further classified into an extrinsic moving least-square (MLS) enrichment and an extrinsic PU enrichment. The ability of the model in capturing crack branching differs with the methods it combines, detailed explanations will be given in Section 4.2.

Cracking particles methods. In the cracking particles method (CPM), the crack is modelled by a set of discrete cracks. As shown in Fig. 12, the discrete crack is restricted to lie on the particles. Since the crack is described by the set of cracked particles, no representation of the crack's topology is needed [75–77]. The method was first developed by Rabczuk and Belytschko [75]. In the model implemented with the cracking particles method, the displacement approximation is given by:

$$\mathbf{u}^h(\mathbf{x}) = \sum_{i\in N} \hat{N}_i(\mathbf{x})\mathbf{u}_i + \sum_{i\in N_c} N_i(\mathbf{x})S(f_i(\mathbf{x}))\mathbf{q}_i \tag{10}$$

where $\mathbf{u}_i$ is the displacement vector, N and N_c are the total set of nodes in the model and the set of cracked nodes respectively; $\hat{N}_i$ and N_i are the continuous and discontinuous shape functions, respectively; $S(f_i(\mathbf{x}))$ is the sign function defined as 1 and -1 on two sides of the crack parametrized by $\mathbf{q}_i$. Therefore, the displacement jump across the crack can be obtained from Eq. (10):

$$[[\mathbf{u}]] = 2\sum_{i\in N_c} N_i(\mathbf{x})S(f_i(\mathbf{x}))\mathbf{q}_i \tag{11}$$

A discrete crack is introduced whenever a cracking criterion is met at a particle [75]. The cracking criteria differ with different material properties, e.g. loss of hyperbolicity is used for a rate independent material while loss of material stability is used for a rate dependent material [97]. The reader is referred to [86] for a more detailed description of commonly used cracking criteria.

Based on the original model, Rabczuk and Belytschko [76] extended its application to three dimensional problems, where a continuous crack is represented by a contiguous set of cracked particles. The sphere particles are separated by a crack plane that

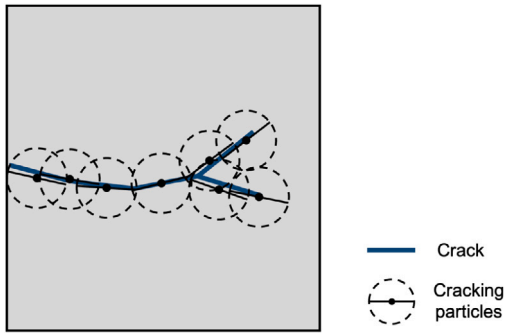

Fig. 12. A schematic illustration of crack branching with CPMs.

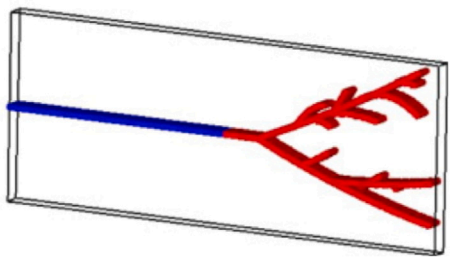

Fig. 13. A 3D example of crack branching with CPMs [76].

passes through the centre of the particle. The method proves its capability in large deformations and arbitrary nonlinear and rate-dependent materials with different examples. A crack branching example in 3D with CPM is given, see Fig. 13. The crack front line is almost linear without capturing the fracture tunnelling feature. The reason may be the use of brittle materials while fracture tunnelling is often observed in ductile materials. Since the crack pattern along the out-of-plane direction is uniform, this example can be considered as a "2.5D" example. To further prove the ability of the method to simulate a real 3D problem, a non-planar crack growth example is given in [76], which is not shown here since this non-planar crack growth example does not include the crack branching phenomenon. Later, Rabczuk et al. [77] further developed the model avoiding the requirement of the enrichment. By splitting particles where the cracking criteria are met into two particles on opposite sides of the associated crack segments, the crack is modelled with no additional degrees of freedom being added in the formulation. By various benchmark examples, the model proves its capability in modelling complex crack patterns in statics and dynamics. Using the CPM, Rabczuk et al. [98] studied the instability in dynamic fracture and reproduced the experimentally observed results, including the limiting velocity, microcrack branching and increase of energy dissipation. It is found that the existence of voids in the model has little effect on the occurrence of microcrack branching. To solve the spurious cracking problems which appear in the original CPM [75], Ai and Augarde [99] improved the crack path curvature modelling through bilinear segments with consideration of cracking angle changes at particles, which allows crack kinks inside a particle. The model was further improved by the so-called "multi-cracked particle method" [100], which can deal with branched cracks (tree-shaped cracks) by splitting a cracking particle multiply. However, all the numerical examples in Ai and Augarde [100]'s work are limited in linear elastic fracture mechanics problems and no dynamic crack branching example is provided. Though solving the spurious cracking problem, the methodology only proves its ability in modelling branched crack (tree-shaped cracks), not the dynamic crack branching process. This is due to the cracking rule it adopted prevents crack branching. The spurious cracking problem was also solved by Xu [101], where a stable CPM based on nodal integration and updated Lagrangian kernels are proposed and a set of simple cracking rules are suggested. Crack branching examples are studied and the existence of limiting velocity observed in dynamic crack branching experiments is proved with the simulation results.

In summary, the CPM is quite suitable for problems with complex crack patterns, especially crack branching. The CPM has the following advantages: (1) no representation of the crack's topology and no crack path continuity are needed; (2) crack branching can happen automatically, no additional branching criteria are needed, and dynamic instabilities related to micro-branches can be captured; (3) it is easily implementable in 3D; (4) no mesh orientation problem. On the limitation side, it is noted that: (1) due to the "discontinuous" representation of the crack surface, special techniques are required to solve the "spurious cracking" problems; (2) since the crack path is approximated via a collection of cracking particles, a finer node distribution is required to increase the accuracy of the model, which may increase the computational cost.

Cohesive zone models. The cohesive zone model (CZM) is developed to describe the nonlinear behaviour during material failure. It assumes a process zone ahead of the real fracture [102,103], where a traction–separation law controls the variation of cohesive traction with the separation (width) of the crack. When the maximum principal stress reaches the cohesive strength of the material

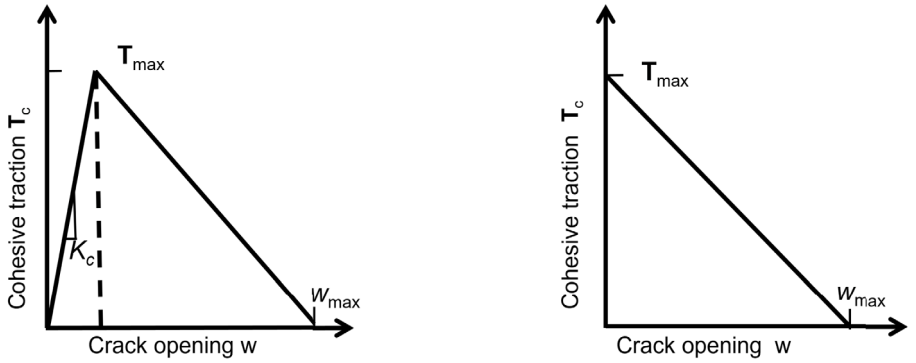

(a) Traction-separation laws for intrinsic CZMs.

(b) Traction-separation laws for extrinsic CZMs.

Fig. 14. Traction–separation laws for CZMs.

$\mathbf{T}_{max}$, the crack initiates. With the crack opening, the cohesive traction will decrease and once it has decreased to zero, the maximum crack opening w_{max} is obtained and complete separation is reached. There are many types of traction–separation laws, such as the exponential form [103], the polynomial form [104], the bi-linear form [105] and the linear form [106]. Park and Paulino [107] gave a critical review on these laws and theirs physical and numerical properties. Depending on the characteristics of the traction–separation law, the CZMs can be divided into two groups: the intrinsic and extrinsic CZMs. As shown in Fig. 14. In the intrinsic CZM, the cohesive traction first increases with the crack opening at an initial stiffness K_c, while the extrinsic CZM does not have the initial stiffness.

Since the CZM is generally a concept to describe the nonlinear behaviour in the process zone, it can be incorporated with different numerical methods and crack models [79]. For example, it can be employed in XFEM and phase field model by introducing a length scale. For discrete cracks in a finite element context, cohesive interface elements (elements equipped with a traction–separation law) have been employed extensively. The simulation process of crack branching modelling with CZMs using cohesive interface elements is further discussed in the following paragraphs.

To model crack branching with the intrinsic CZM, the deformation equation first needs to be given and the domain needs to be divided into elements. Then, cohesive interface elements need to be assigned on all finite element surfaces before simulation. Finally, the displacement field is solved with the traction–separation law. During this process, remeshing is not required and the crack is allowed to propagate along element boundaries. No external criterion is needed for crack branching since the branching phenomenon emerges as a natural outcome of the initial–boundary value problem solution [73]. However, because the finite initial slope of the traction–separation law modifies the stiffness of the structure and alters the wave propagation, the intrinsic CZM has issues such as the artificial softening effect, loss of consistency, spuriously high crack velocity (the lift-off issue) (see [108] for a complete discussion about these issues). A remedy to reduce the effect of artificial compliance is to increase, if possible, the initial elastic slope of the traction–separation law, which results in severe stable time step restrictions and may even render the intrinsic approach unsuitable for explicit dynamic calculations, or in ill-conditioning of the tangent stiffness matrices in static or implicit dynamics analyses.

The process for modelling crack branching with the extrinsic CZM is similar to the intrinsic CZM. The difference lies in the cohesive interface elements, which is illustrated in Fig. 15. Instead of inserting all cohesive interface elements first, cohesive interface elements will be assigned adaptively when the criterion (the cohesive traction reaches the cohesive strength $\mathbf{T}_{max}$) is satisfied [74]. By doing so, it avoids the artificial softening effects, however, additional issues of the efficient parallelization of extrinsic cohesive interface elements with the change in mesh topology need to be addressed. In addition, the extrinsic CZM has the time discontinuity issue (the traction before and after insertion/activation of an interface element may not be continuous). This is because before cracking, the cohesive traction depends on the stress field within the neighbouring continuum elements while in the subsequent time step following cohesive element insertion, the cohesive traction relies on the cohesive law [108]. The time discontinuity leads to oscillatory behaviour, non-convergence in time and dependence on nonphysical regularization parameters [109]. To solve this, different approaches have been proposed to make sure the time continuity condition (the continuity of traction before and after insertion/activation of an interface element) is satisfied [109–111].

Both intrinsic CZMs and extrinsic CZMs have the problem of mesh dependency and bias since the cracks are only allowed to propagate along element facets. Arias et al. [112] modelled the macroscopic crack branching with the extrinsic approach and concluded that the occurrence of branching may be very sensitive to the mesh parameters. Due to the dependence on mesh, the crack paths predicted tend to be somewhat inaccurate. The problem can be remedied by finer mesh or special mesh operations. Agwai et al. [113] found that finer and unstructured mesh performs better than coarser and structured mesh in predicting the branching pattern observed experimentally by investigating the different levels of mesh refinement for both structured and non-structured meshes. Special operations, such as nodal perturbation and edge-swap topological operation [114], splitting of polygonal finite elements [115,116], stress recovery and domain integral [117] are also proposed to reduce and remove mesh bias and dependency in CZMs, by which physical phenomena associated with dynamic crack branching are successfully captured.

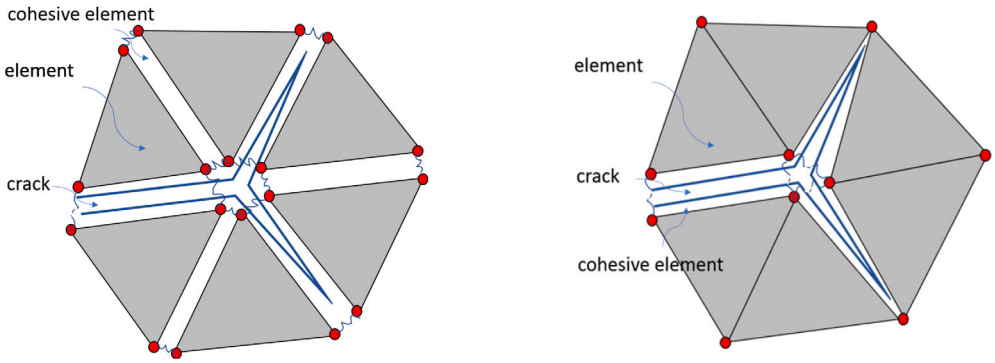

(a) Crack branching with intrinsic CZMs. (b) Crack branching with extrinsic CZMs.

Fig. 15. Crack branching with CZMs.

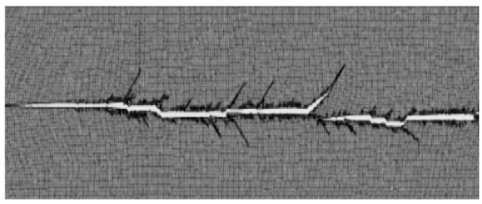

Fig. 16. A 2D example of crack branching with CZMs [118].

Many successful applications can be found in modelling crack branching using CZMs. With the intrinsic CZM, Xu and Needleman [73] successfully modelled the crack branching phenomenon. The results show that the branching phenomenon has a close relationship with the applied loading and the dynamic crack velocity computed by the intrinsic CZM is in good agreement with experimental observations. By using an advanced topological data structure representation, Zhang et al. [118] presented the extrinsic cohesive modelling of dynamic fracture and emphasized the importance of adopting the extrinsic CZM for the simulation of multiple micro-branches where the results yield improved agreement with experimental results compared to Miller et al. [119], which employs a potential-based intrinsic CZM for the same problem. As shown in Fig. 16, complex crack branching patterns including both multiple branches and micro-branches are predicted. After investigating the micro-branching process, the numerical results reveal that the increased energy input leads to increased crack surface roughness, longer micro-branches and higher crack speed. Paulino et al. [114] proposed an extrinsic cohesive zone model using nodal perturbation and edge-swap operators and proved the capability of the model in providing consistent results between experiments and computational simulation in terms of microbranching patterns and crack velocity. Park et al. [120] proposed adaptive mesh refinement and coarsening schemes for efficient computational simulation of dynamic cohesive fracture, which successfully captures small branches observed experimentally before the crack branching. It is shown that the formation of micro-branches leads to a lower main crack velocity, which is closer to experimental observations. Though this work uses an advanced topology-based data structure to store the FE discretization and realize parallelization, examples in three dimensions are not given due to the complexity of the implementation of the extrinsic approach. For more complex problems like dynamic fracture propagation in three dimensions, the hybrid discontinuous Galerkin cohesive element method has been adopted [121]. The cohesive interface elements are assigned first on all element surfaces before simulation and are not allowed to open by a discontinuous Galerkin formulation. The model is then switched to the extrinsic cohesive crack model when a failure criterion is met. The method is capable of modelling large-scale dynamic crack propagation in three dimensions with powerful computers since it saves from the trouble of extensive updating of mesh information and avoids issues that intrinsic cohesive interface elements bring. Radovitzky et al. [110] presented a scalable 3D fracture and fragmentation algorithm based on the hybrid discontinuous Galerkin and cohesive element method and demonstrated its ability in capturing intricate patterns of cracks including branching. Becker and Noels [122] presented a full-Discontinuous Galerkin formulation of nonlinear Kirchhoff–Love shells and combined it with CZMs to perform thin body fracture simulations. Three-dimensional simulations including crack branching are given, see Fig. 17. Baek et al. [123] proposed a computational framework for multiscale dynamic fracture analysis, where micro-scales and macro-scales are integrated by introducing an adaptive microstructure representation. A Park–Paulino–Roesler (PPR) potential-based CZM was presented in [124,125], which yields a consistent traction–separation relationship for an arbitrary separation path [126]. The self-interpenetration during dynamic fracture simulation was avoided by employing a simple penalty method [127] and the nonlinear dynamic fracture behaviour associated with spontaneous multiple microcrack initiation and branching in conjunction with the microstructure was investigated. The results show that the microstructure should be carefully considered for dynamic cohesive fracture investigations.

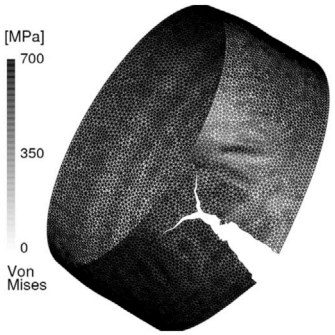

Fig. 17. A 3D example of crack branching with CZMs [122].

In summary, the CZM is a good choice for the study of dynamic crack branching and can be combined with different models and methods to describe the nonlinear behaviour of the crack. With cohesive interface elements, it is easily incorporated into a finite element framework and has the ability of detecting crack initiation and capturing multiple branches and micro-branches. The mesh dependency problem it suffers can be solved by refining meshes or other special mesh operations, which in turn, may increase the computational cost and complexity of implementation procedure, especially in 3D. A promising approach to avoid these problems is the combination of the cohesive law and the discontinuous Galerkin formulation. Explanations about the approach and its application in dynamic fractures including branching can be found in [108,110,121–123,128].

4.1.2. Smeared crack models

Phase field models. As a recently emerged model, the phase field model (PFM) smears the crack over a certain domain without tracking the crack surfaces. Based on the principle of minimum total potential energy, the PFM solves a fracture problem as an energy minimization problem. The energy functional for simulating crack propagation is first given by Francfort and Marigo [129]:

$$E(\mathbf{u}, \Gamma) = \int_{\Omega} \Psi(\epsilon(\mathbf{u}))d\Omega + G_c \int_{\Gamma} d\Gamma \tag{12}$$

where Ω is a domain describing a cracked solid, Ψ denotes the elastic energy density, $\epsilon(\mathbf{u})$ is the strain field, and G_c is the fracture toughness, which yields an admissible crack set $\Gamma \subset \Omega$. $\mathbf{u}$ is the displacement field and is discontinuous across Γ. Bourdin et al. [87] devised its regularized formulation:

$$E_{\epsilon}(\mathbf{u}, \phi) = \int_{\Omega} f(\phi)\Psi(\epsilon(\mathbf{u}))d\Omega + G_c \int_{\Omega} (\frac{1}{4l_0}(1-\phi)^2 + l_0|\nabla\phi|^2)d\Omega \tag{13}$$

where ϕ is damage-like crack phase-field parameter with 1 representing the unbroken part and 0 the totally broken part. $f(\phi)$ is the energetic degradation function to help prevent numerical difficulties where the material is broken (e.g. $\phi = 0$). The width of transition zone is controlled by the length scale l_0. When l_0 is very small, the diffusive crack presented by the phase field would approximate a sharp crack solved in discrete crack approaches. With the help of Eq. (13), the scalar field (the phase field) turns the intact material into a broken material smoothly instead of treating cracks as strong discontinuities. This enables PFM to overcome difficulties in modelling complex crack problems in three dimensions with traditional numerical methods. Because the propagation of the crack is obtained through the solution of the differential equation, the PFM also avoids the need of additional criteria for crack propagation and additional work to track the fracture surface algorithmically [88,130].

The ability of PFM to simulate crack propagation and branching in two and three dimensions has been demonstrated [88,131–135]. Borden et al. [88] extended the quasi-static phase-field crack model to a dynamic model and used both 2D and 3D crack branching examples to show that the combination of the phase-field model and local refinement strategy is an effective method for simulating complex crack problems. Hofacker and Miehe [131] established a phase field model based on variational principle and demonstrated its performance by means of representative 2D and 3D quasi-static and dynamic model problems including branching. Bleyer and Molinari [132] investigated the microbranching instability occurring in dynamic crack propagation with a 3D variational phase-field model and showed that the microbranching process is a three-dimensional instability and the branching patterns are strongly influenced by phase-field internal length scale. To overcome the limitations of the strong dependence of crack branching patterns on internal length scale, a regularized phase field based cohesive model was introduced by Wu and Nguyen [133],Wu [134], Nguyen and Wu [135], which is insensitive to the length scale and capable of capturing multiple crack branching.

Compared with remeshing models which need the separation between the elements to describe the crack surface, PFMs are capable of modelling multiple branches, widening of damage zone (fracture roughness) and micro-branches. Regarding multiple branches, Zhou et al. [136,137] and Ren et al. [138] presented PFMs for simulating complex crack patterns. Multiple crack branches phenomenon is observed, which demonstrates the advantages of PFM in modelling complex crack propagation in rocks. Regarding micro-branches, it refers to the branch of which length is in order of length-scale of simulation [34]. Fig. 19 shows a 3D crack branching example with micro-branches based on PFM. From the figure, a slightly curved crack front (the crack tunnelling feature)

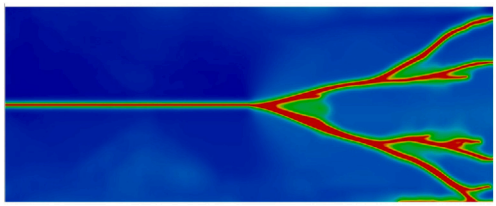

Fig. 18. A 2D example of crack branching with PFMs [144].

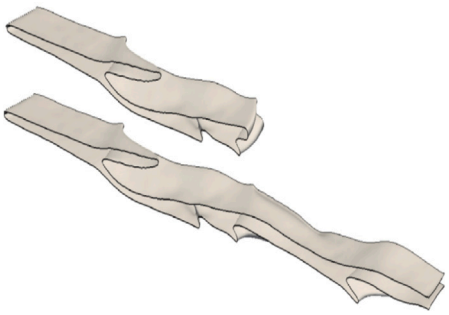

Fig. 19. A 3D example of crack branching with PFMs, showing isosurfaces of phase field at $\phi = 0.3$ [145].

and slightly rough crack surfaces can be observed. Regarding the widening of the damage zone before branching, it can be seen as an increase in fracture surface roughness prior to branching, which has been observed in experiments [4]. According to the branching mechanism proposed by Ravi-Chandar and Knauss [12,13,14], a widening damage process-zone appears before crack branching due to the increasing fracture roughness (mirror-mist-hackles transition). Then, after branching, as the crack branches go on propagating, the damage zone become "thinner", indicating that the crack surfaces turn smooth again. If the energy provided is sufficiently high, the "widening-thinner process" is repeated, and secondary branches can be observed. Fig. 18 shows a 2D crack branching example, where the widening of the damage zone before branching and multiple branches can be observed.

Given its strong ability in modelling crack branching without remeshing and external criteria, more authors choose to apply PFM for the study of the dynamic crack branching aiming at providing new analyses of the mechanisms behind this phenomenon. The crack velocity, the crack branching angle, the crack branching criterion, as well as the sensitivity of numerical simulation parameters to crack branching are studied.

In terms of the crack velocity, since the crack tip is not uniquely defined in PFM [131], a number of approaches are proposed to measure the crack tip position. Borden et al. [88] proposed to calculate the propagation velocity explicitly by finding the crack tip with a certain defined phase-field value. Wu et al. [139] computed the crack speed from using the slope of the line that best fits the three points, in a least square sense. Hofacker and Miehe [140] tried to obtain the velocity implicitly by using the crack surface velocity to represent the crack speed. All of the approaches are reasonable due to the definition of the crack tip position being physically implicit in PFM. Regarding the branching angle, similar conclusions are made by Wu et al. [139], Hofacker and Miehe [140] that with increasing loading amplitude or velocity, the crack branches earlier and the branching angle gets smaller. Various branching criteria have been examined. Henry [141] studied crack propagation in two dimensions using the PFM and believed that the branching instability starts with a critical speed of $0.48c_S$, where c_S is the shear wave speed. Wu et al. [139] denied the validity of the velocity branching criterion by proving that crack speed at the moment of branching is very sensitive to the width of the sample with a 2D PFM model. Instead of crack velocity, Hofacker and Miehe [140] preferred the phase field velocity and the crack surface velocity as local and global indicators for branching. Through studying the limiting velocity, crack branching and velocity-toughening mechanisms with the PFM, Bleyer et al. [34] proposed that the branching occurs when the local energy release rate exceeds twice the critical energy release rate. By quantifying the energy flux into the crack tip and fracture energy, Tian et al. [142] confirmed that the crack bifurcation obeys an energy criterion as it is observed that the crack bifurcation of PMMA always occurs with the energy flux into the crack tip exceeding a critical value. Mandal et al. [143] systematically analysed mesh convergence and length scale sensitivity in dynamic crack simulation with PFMs. Quantitative evaluation of branching angles and crack tip velocity and comparison between PFM simulation results and experimental results are provided.

The crack branching phenomenon is very sensitive to numerical simulation parameters. For example, the solution scheme is influential, e.g. the monolithic scheme and the staggered scheme may lead to different crack patterns [146] and different branching moment [147]. The mesh size is also a significant factor, e.g. multiple crack branches can only be captured by sufficiently refined meshes while a different mesh size may result in different branching time [131,139,140,147,148].

The sensitivity of the branching phenomenon to the mesh size leads to limitations of PFM. The computational cost will increase since the mesh needs to be fine enough for the phase field to represent the accurate position of the crack. However, PFM is a

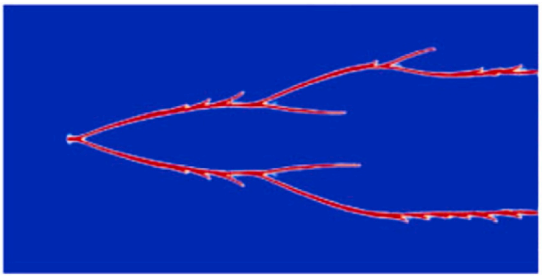

Fig. 20. A numerical example of crack branching with nonlocal models [151].

very promising model for crack branching studies with the following advantages: (1) no need for initial crack length settings and no external criteria for branching since the crack patterns can be automatically captured by solving the equation based on energy minimization; (2) straightforward implementation in three dimensions; (3) capable of modelling multiple branches, widening of damage zone (fracture roughness) and micro-branches.

Nonlocal models/gradient models/viscous models. When modelling failure caused by progressive distributed damage, the material exhibits strain-softening and the governing differential equations may lose ellipticity, which renders the boundary value problem ill-posed and causes physically meaningless, mesh-dependent finite element results [149]. To solve these problems, non-local models, gradient models and viscous models are commonly employed. By introducing a characteristic length into the discretization, these models "smear" the crack over a certain domain involving several elements and avoid representing the crack topology and crack tracking algorithms [91].

An integral-type nonlocal model is defined as a model in which the constitutive law at a point of a continuum involves weighted averages of a state variable over a certain neighbourhood of that point [89]. The integral formulation in the model allows the introduction of a characteristic length that qualifies the neighbourhood over which the parameters/calculated numbers get "smeared" over. The gradient models can be constructed by including higher-order gradients directly in the damage loading function [150]. The higher-order gradients can be employed to smooth the non-uniformity or singularities in the strain field when regularization of singularities or discontinuities is required. The viscosity models can be regarded as introducing higher-order time derivatives and a length scale associated with the viscosity is employed, which also restore the well-posedness of the BVP or initial BVP [91]. Detailed explanations of these models are given in literature [89–91], here we mainly focus on the performance of these models in modelling and investigating dynamic crack branching.

Examples for the application of nonlocal models and gradient models to dynamic crack branching problems can be found in [151,152]. With an integral-type nonlocal continuum damage model, Wolff et al. [151] conducted simulations of dynamic crack branching in PMMA and studied the dynamic crack branching instabilities. It is found that the selection of the rate-dependence damage law and the critical strain for damage initiation are necessary to predict crack patterns, crack tip velocities and dissipated energies accurately. A figure of crack branching with the integral-type nonlocal continuum damage model is shown in Fig. 20. It can be observed that just like PFM, the nonlocal models are also capable of capturing the multiple branches, widening of damage zone (fracture roughness) and micro-branches. Wang et al. [152] proposed a localizing gradient damage model with micro inertia effect for modelling dynamic fracture propagation in quasi-brittle materials, which resolves the mesh sensitivity issue and spurious damage growth appeared in conventional gradient damage models and shows good performance in reproducing crack patterns (from a straight crack to sub-branching, and finally to macro branching), crack velocities, and fracture energies observed in the experiments.

The advantages of the nonlocal models, gradient models and viscous models are manifold: (1) representation of the crack topology and crack tracking algorithms are avoided; (2) the issue of mesh dependency and additional criteria to control crack branching are avoided; (3) they are capable of modelling crack surface roughness and micro-branches. Their limitations lie in that (1) physical inconsistencies may appear in the characterization of crack kinematics due to the wrong selection of related parameters, e.g. parameters for rate-dependence damage law; (2) computational cost may significantly increase due to the increase of mesh density to get a more accurate prediction of the crack.

4.2. Numerical methods

Numerical methods are employed to solve the equations of the bulk material. According to whether spatial derivatives are employed or not, the numerical methods can be further classified into continuum methods and discontinuum methods. The simulation of crack branching is a highly challenging problem due to its complexity. Difficulties if classified according to the simulation process are divided into three aspects: pre-branching, during branching and post branching. In pre-branching moving singularities at the tips of cracks should be treated accurately and a branching criterion should be detected to decide the branching time for a crack [153]. During branching a criterion or a mechanism is required to predict the crack path, including the branching patterns and branching angles. In post-branching, the redistribution of energy and the influence of different branches need consideration. Until now, numerous methods have been applied to the modelling of crack branching with varying success. A superior method should have the following characteristics to better capture the phenomenon of crack branching:

Table 3
Numerical methods for crack branching simulation.

Numerical methods	Advantages	Limitations
FEM	Flexible and robust	Remeshing is required if the adaptive FEM-based model is used, which is difficult in 3D
XFEM	Independent of mesh	Needs special enrichment for junctions and branches
BEM	Reduces dimensions	Not well-suited for nonlinear problems
MMs	Eliminate difficulties mesh-based methods brings	Have boundary implementation, instability, numerical integration of the weak form, high computational cost issue
PD	Avoids remeshing	Has relatively high computational cost and difficulties in dealing with boundary conditions
DEM	Well-suited when considering heterogeneity	Limited in granular materials, awkward in predicting macroscopic properties and has relatively high computational cost

- The ability of capturing different crack branching patterns, including macro crack bifurcation, micro-branches, a single crack with multiple branches and multiple cracks with branches.
- Good agreement with the experimental results and theoretical prediction in branching features, such as branching angles and the crack velocity.
- Relatively easy and robust implementation process with affordable computational cost.

Specifically from the view of crack branching, this section summarizes and compares different numerical methods. For each method, the physical and mathematical principles are first introduced, followed by the explanation of crack branching simulation, after which historical and state-of-the-art applications in crack branching simulation are summarized with discussions of both advantages and limitations, see Table 3. The emphasis differs in applications of different methods, for example, focusing more on verification (using various branching examples to prove the superiority of the models built by the improved numerical methods) or focusing more on the analysis (analysing the mechanism behind the crack branching phenomenon with these models).

4.2.1. The continuum methods

The finite element method. The idea behind the finite element method (FEM) is to break the continuum into a number of simple geometric elements and estimate the characteristics of the continuous domain by assembling the similar properties of discretized elements per node [154]. The method is suitable for modelling bulk materials. It has been applied to a wide range of crack problems [155] and can be combined with nearly any crack model due to its flexibility and robustness, see Fig. 7.

In this section, depending on how the branching is simulated, a commonly used adaptive FEM-based model (FEM combined with remeshing models) is discussed. Note that the term "adaptive FEM-based model" in this section does not include the models based on both finite element method and cohesive elements, which are discussed in Section 4.1. The simulation process of crack branching using the adaptive FEM-based model mainly includes the establishment and solution of the deformation equation, the selection of the propagation criterion, and the meshing strategy. By establishing and solving the deformation equation, the crack footprint can be obtained. Since the crack branching process is dynamic, the inertial force and the acceleration terms need to be considered. Here the Newmark method [156] is used to solve the governing equations and the resulting system is given below:

$$(a_0\mathbf{M}+\mathbf{K})\{\mathbf{u}\}^{n+1}=\{\mathbf{F}\}^{n+1}+\mathbf{M}(a_0\{\mathbf{u}\}^{n}+a_2\{\dot{\mathbf{u}}\}^{n}+a_3\{\ddot{\mathbf{u}}\}^{n}) \tag{14}$$

$$\{\ddot{\mathbf{u}}\}^{n+1}=a_0(\{\mathbf{u}\}^{n+1}-\{\mathbf{u}\}^{n})-a_2\{\dot{\mathbf{u}}\}^{n}-a_3\{\ddot{\mathbf{u}}\}^{n} \tag{15}$$

$$\{\dot{\mathbf{u}}\}^{n+1}=\{\dot{\mathbf{u}}\}^{n}+a_6\{\ddot{\mathbf{u}}\}^{n}+a_7\{\ddot{\mathbf{u}}\}^{n+1} \tag{16}$$

where $\{\ddot{\mathbf{u}}\}$, $\{\dot{\mathbf{u}}\}$, $\{\mathbf{u}\}$, $\{\mathbf{F}\}$ are the global vectors of nodal acceleration, nodal velocity, nodal displacement and nodal load, respectively; the superscript n represents time step, $\mathbf{M}$ and $\mathbf{K}$ are the mass matrix and the stiffness matrix, respectively. The coefficients a_0 - a_7 are the parameters in the Newmark method [2].

The next step is to determine whether the crack will branch or not. The branching criterion for the adaptive FEM-based model can only be an external criterion (see Section 3.2.1), which increases the difficulty of the simulation. The branching time, the branching angle and the branching velocity need to be determined. Due to the singularity of the crack tip, determination of appropriate physical mechanisms and formula to calculate the associated parameters remains a challenge.

After obtaining the crack footprint, the mesh needs to be updated. It is possible to model one or two branches, but as more branches develop, remeshing becomes very complex. Both the singularity at the crack tip and the small angle between crack branches require a heavily refined mesh and may result in a large increase in computational cost.

To the best of the authors' knowledge, there do not appear to be many examples using the adaptive FEM-based model to simulate crack branching due to its implementation complexity. Nishioka et al. [2] modelled the dynamic crack branching phenomenon with a moving FEM (adaptive meshes) based on Delaunay triangulation and a switching method using the dynamic J-integral. The moving

FEM has the advantage of exactly satisfying the boundary conditions in front of and behind the propagating crack tip dynamically. The switching method using the dynamic J-integral provides an accurate way of evaluating the dynamic J-integral regardless of crack path, which is especially applicable when the crack tips are very close to each other after branching. The generation of dynamic crack branching phenomenon in Homalite-911 is successfully modelled and the numerical results agree well with experiments [2]. However, only examples for a crack with two branches are presented and for more complicated crack branching patterns are not discussed. Using a further developed remeshing strategy, Tchouikov et al. [66] investigated more complicated crack branching problems including multiple crack bifurcation. A comparison between numerical and experimental results was provided but the calculation efficiency was not mentioned. We conclude that the adaptive FEM-based model still faces challenges when dealing with crack branching as discussed above, especially in three dimensions.

The extended finite element method. In order to solve mesh dependency problems, the extended finite element method (XFEM) was developed [84,85]. Similar to FEM, it is suitable for modelling bulk materials. To simulate crack propagation, XFEM uses the enriched shape function with discontinuous features to represent the discontinuity [157]. By doing so, the displacement discontinuity can be captured and the crack can propagate on any surface within one element instead of along element boundaries. Thus, remeshing and mesh dependency issues appearing in discontinuous problems with FEM can be overcome. However, the use of enrichment functions also brings the issue of incompatibility between accuracy of the solution and conditioning of the system matrix, especially when solving large 3-D problems. The condition numbers of the stiffness matrix can be worse if one utilizes enrichment functions, and thus it can affect the accuracy of the solution. Several studies have attempted addressing this issue [158–160].

Generally, there are two ways to enrich an approximation: intrinsic enrichment (enriching the basis vector) and extrinsic enrichment (enriching the approximation) [161]. The idea for intrinsic enrichment is to enhance the approximation space by building new basis functions which are derived from a specific problem into the standard approximation space. For instance, the asymptotic near tip displacement field can be built into the basis functions so that the singularities at the crack tip can be represented. For extrinsic enrichment, the enrichment functions are added to the standard approximation in specific zones, and as a result, the computational cost is reduced.

Though the characteristic of XFEM facilitates its application in modelling internal or external boundaries such as holes, inclusions, or cracks, the simulation process of crack branching with XFEM is not an easy task. First, appropriate enrichment schemes need to be considered for the element with the crack branch junctions and crack branches. Secondly, though the computational cost is less expensive without remeshing, the simulation process still requires external branching criteria, bringing issues such as the decision of reliable criteria and the calculation of related crack parameters. Thirdly, XFEM typically uses the level set method to track fractures, but as fracture branches increase the associated operation becomes increasingly complicated, especially in 3D cases. In the context of the crack branching problem, the displacement approximation $\mathbf{u}^h$ with the partition of unity is expressed as [162]:

$$\mathbf{u}^h(\mathbf{x}) = \sum_{i\in N} \mathbf{u}_i N_i + \sum_{j\in N^H} \boldsymbol{\alpha}_j N_j H(\mathbf{x}) + \sum_{k\in N^C} N_k \left(\sum_{\alpha=1}^{4} \boldsymbol{\alpha}_k^{\alpha} \Phi_{\alpha} \right) + \sum_{m\in N^J} \boldsymbol{\alpha}_m N_m J(\mathbf{x}) \tag{17}$$

where $\mathbf{u}_i$ is the vector, N_i, N_j, N_k and N_m are the standard finite element shape functions associated with node i, j, k and m respectively; $\boldsymbol{\alpha}_j$, $\boldsymbol{\alpha}_k^{\alpha}$ and $\boldsymbol{\alpha}_m$ represent the nodal enriched degrees of freedom associated with the Heaviside function $H(\mathbf{x})$, near tip asymptotic field function Φ_{α} and junction function $J(\mathbf{x})$, respectively; N^H, N^C and N^J are the set of nodes to enrich for the crack, crack tip and junction.

Progress has been made on modelling the crack branching with XFEM. Daux et al. [162] developed a methodology to construct the enriched approximation based on the interaction of the discontinuous geometric features and calculated the SIF of static cracks with multiple branches. This can be used for static cracks, but the propagation of the dynamic crack branching process is not taken into consideration. To improve the modelling of dynamic crack propagation by XFEM, Belytschko et al. [163] developed a new methodology for treating elements that contain crack tips, which allows the velocity field of the element containing the crack tip can change smoothly from a partially cut element to a fully cut element. The crack path and velocity can be determined directly by the loss of hyperbolicity criterion, which facilitates the modelling of dynamic crack growth problems, including crack branching. However, only a relatively simple bifurcation phenomenon is captured, while fracture roughness and micro-branches cannot be captured, see Fig. 21. To seize the discontinuity around the junction of a branched crack, Xu et al. [58] introduced the enrich scheme of the element crossed by two separated cracks, the element embedded by a junction, and the way of constructing the diagonal mass matrix for the branched element, with which the initial branching process of a moving crack (the main crack develops two branches) is successfully simulated. However, this method requires an increase in additional degrees of freedom. For more complex branching problems with increasing degrees of freedom in one element, Chen and Zhou [164] proposed an enhanced XFEM coupling the phantom node method [165] and proved its robustness and accuracy in handling the complex branched crack problems. To capture complicated discontinuity patterns, Song and Belytschko [166] introduced a hybrid discontinuity tracking-fitting method that fits cracks with discrete discontinuities at nodes based on the XFEM. This method is quite similar to the cracking particles method, which is capable of modelling complicated fracture patterns since it needs no explicit representation of the crack's topology.

In summary, the XFEM possesses the following advantages: (1) lower computational cost without the need of remeshing; (2) suitable for cracks with complex geometry or problems with geometric nonlinearities because of mesh independence. These advantages make the XFEM become a powerful and promising tool in the simulation of complex crack problems. However, the XFEM has imitations when dealing with multiple interacting and branched cracks and micro-branches, since the computational cost increases as the number of cracks grows and its formulation becomes increasingly complex. For branches or junctions, special discontinuous displacement enrichment needs to be developed and external criteria for the injection of the enrichment are needed. Additionally, because of the lack of a reliable crack branching criterion, prediction of crack propagation and branching remains a challenge [91].

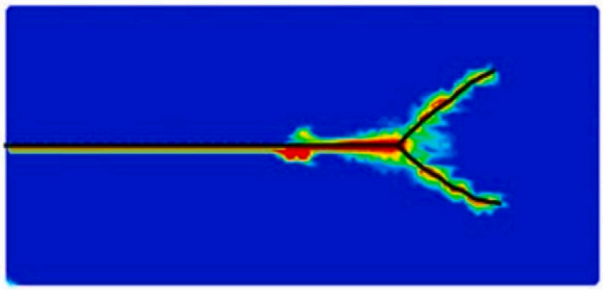

Fig. 21. A numerical example of damage for crack branching with XFEM [163].

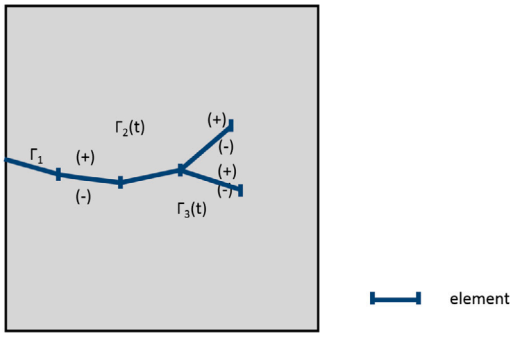

Fig. 22. A schematic illustration of crack branching with BEM.

The boundary element method. The boundary element method (BEM) is also widely used in crack simulations due to its ability to automatically follow the propagation of the crack with limited remeshing and its inherent accuracy [167]. The BEM is designed for solving boundary value or initial value problems and formulated in terms of boundary integral equations [168]. Similar to the FEM, the BEM is suitable for modelling bulk materials. Instead of discretizing the whole domain into volume elements, the BEM only discretizes the domain boundary for interpolation approximation. The basic process of modelling crack propagation with BEM is slightly different from FEM. The mathematical model needs to be established first, then the boundary integral equations can be obtained by taking boundary values in the representation formula. After generating the system of discrete equations by collocation, Galerkin's method or the least squares method, the displacement field can be solved. During this process, crack parameters related to the external propagation criteria, such as stress intensity factor and energy release rate, need to be calculated to determine crack development. The calculation of these parameters is much simpler than FEM due to the reduced dimensional features of BEM. Once the crack develops, remeshing is needed by adding the elements at the end of the crack tip without changing the remaining mesh.

The displacement integral equation at an interior point $\mathbf{X}$ in the absence of a body force for linear elastic crack problems is given by [167]:

$$\mathbf{u}_i(\mathbf{X}) = \int_{\Gamma_S+\Gamma_n^+ +\Gamma_n^-} \mathbf{U}_{ij}(\mathbf{X},\mathbf{x}) \cdot \mathbf{t}_j(\mathbf{x}) d\Gamma - \int_{\Gamma_S+\Gamma_n^+ +\Gamma_n^-} \mathbf{T}_{ij}(\mathbf{X},\mathbf{x}) \cdot \mathbf{u}_j(\mathbf{x}) d\Gamma \tag{18}$$

where Γ_n^+ and Γ_n^- represent the upper and lower crack surfaces, respectively, and Γ_S represents the outer boundary, $\mathbf{u}_j$ and $\mathbf{t}_j$ denote the boundary displacement and the traction, respectively; $\mathbf{U}_{ij}$ and $\mathbf{T}_{ij}$ are the fundamental solutions for displacement and traction, respectively. Fig. 22 shows a schematic illustration of crack branching simulated by BEM.

The difficulties of BEM for fracture problems reside in the coincidence of crack nodes, giving rise to a singular system of algebraic equations. Different techniques such as the sub-region boundary element method (SBEM), displacement discontinuity methods (DDM), dual-boundary element method (DBEM) and dual-reciprocity boundary element method have been developed to solve this problem [92]. Seelig and Gross [169] presented a pioneering work of modelling dynamic crack branching with BEM, where crack growth and branching criteria were combined and a time-domain boundary integral equation system was established. The crack propagation speed and the SIF were calculated, showing good agreement with the experimental observations. Since then, examples for BEM simulation of crack branching have been presented in the literature [64,170–175].

Branching examples are used to verify the improvement and accuracy of the proposed schemes. For example, Rajapakse and Xu [170] presented a complete set of piezoelectric Green's functions in closed form and developed a solution scheme based on the boundary integral equation method to analyse plane cracks in piezoelectric solid. A double-branched crack model is used to verify this scheme. Yan [171] tried to place the crack-tip displacement discontinuity elements at the corresponding crack tip on top of the constant displacement discontinuity elements that cover the entire crack surface. By using such elements and the SIF as a

propagation criterion with a known branching angle, complex crack problems including a branched crack example are employed to demonstrate the efficiency and accuracy of the proposed method. Santana and Portela [173] applied the dual boundary element method (DBEM) to the analysis of mixed-mode multiple-crack growth including branching cracks, where the SIF was evaluated via the J-integral and the incremental analysis was used to define the direction and the extension of multiple interacting cracks. Other approaches focus on the study of the physical mechanisms behind the branching phenomenon. Rafiee et al. [64] investigated fast running cracks branching under different bi-axial loading conditions. It is found that branching depends on the opening mode SIF, the crack velocity, and the orientation on the maximum circumferential stress in the vicinity of the crack tip. Marji [172] modelled the crack branching process by using an indirect BEM specially developed to treat the kink points of propagating cracks in brittle solids and studied the mechanism of secondary crack initiation and propagation. The results show that the formation of the wing crack and the secondary crack caused by the crack tip and the crack kink point may lead to a quasi-static crack bifurcation process. Fedelinski [174] applied the BEM to the analysis of the branched and intersecting cracks in statically and dynamically loaded plates. The influences of angles between branches of the crack and dimensions of the plate for the star-shaped crack on a dynamic SIF were analysed. Shrivastava et al. [175] presented a hydraulic fracture model with a three-dimensional displacement discontinuity method and investigated the interaction between multiple cracks and branches. The heterogeneity of solid rocks is one reason for crack branches, which further results in a complex fracture network.

The BEM offers clear advantages. The stress field in the vicinity of the crack tip can be accurately calculated and the computational efficiency can be greatly increased due to the reduction of the dimension. Nevertheless, it still suffers from the inability to model crack propagation and branching autonomously as it needs external criteria. Besides, the application of BEM in nonlinear problems is limited, as it still requires that the fundamental solution is expressed in terms of Green's functions [91].

The meshfree methods. When dealing with crack branching problems, the traditional FEM has the limitation of remeshing, which is time-consuming especially in 3D. The XFEM avoids the need of remeshing, however, it is awkward when dealing with multiple interacting and branched cracks, since the computational cost increases as the number of cracks grows and its formulation becomes increasingly complex. Meshfree methods (MMs) were devised with the objective of eliminating part of the difficulties associated with reliance on a mesh to construct the approximation [176], providing an advantage in dealing with crack growth problems.

In general, MMs refer to numerical techniques that do not require any predefined mesh information for domain discretization, and they use a set of points scattered within the problem domain as well as on the boundaries of the domain to represent the problem domain and its boundaries [177]. MMs model the bulk material as continuum. Approaches of modelling discontinuities in MMs can be classified into two types generally: methods based on the intrinsic and extrinsic enrichment and modification of the weight function [176]. The second type can be further classified into the visibility method, the diffraction method, the transparency method, and the "see through" and "continuous line" method [86]. Pioneered by Gingold and Monaghan [178], the smoothed particle hydrodynamics method (SPH) was developed on a strong form, while other methods were developed later based on a weak form, among which the element-free Galerkin method (EFGM), reproducing kernel particle method (RKPM), material point method (MPM) are popular approaches [177]. Compared with MMs based on strong forms, the MMs based on weak forms are more robust and steady. Detailed descriptions of these MMs and their classifications, advantages, limitations, and computer implementation aspects can be found in studies by [86,91,176,179–181]. Here, we only give a brief introduction of these MMs and focus more on their ability of capturing crack branching.

SPH is a pure Lagrangian, meshfree method, which was first developed to model hydrodynamic flows and then extended to solid mechanics [182,183]. In SPH, the domain is discretized into particles and each particle interacts with its neighbour particles within its influence domain through a kernel function. Early works on studying crack with SPH can be found in [184–187]. In most of these work, the SPH is based on Eulerian kernels (kernel functions which are expressed in terms of spatial coordinates) and the crack can occur naturally due to separating particles. Compared with the traditional mesh-based methods, it avoids the mesh dependence problem when dealing with cracks. However, it suffers from problems such as spurious instabilities, expensive computational cost and inaccurate crack path prediction [176,188]. To solve these problems, Lagrangian kernels (kernel functions in terms of material coordinates) instead of Eulerian kernel functions are employed [189,190]. However, Lagrangian kernels require specific strategies to deal with fractures since neighbour particles do not change during a simulation. A commonly used strategy is the visibility method, in which the displacement discontinuity is modelled by excluding the particles on the opposite side of the crack in the approximation of the displacement field under the assumption of opaque crack boundary [86]. Recently, a strategy called "pseudo-spring" was developed by Chakraborty and Shaw [191] to facilitate SPH to model crack propagation without any numerical artefact. The crack path can be tracked automatically by the broken pseudo-springs. Using the Pseudo-Spring smoothed particle hydrodynamics method (Pseudo-Spring SPH), Islam and Shaw [192] simulated 2D and 3D crack propagation and branching and studied effects of tensile loading amplitude on crack branching.

The element free Galerkin methods (EFG), first developed by [193], is a method based on moving least-square (MLS) interpolants. The EFG requires only nodal data without the requirement of element connectivity. Compared with SPH, the EFG avoids the calculation of nodal volumes and obtains the gradient fields directly by taking the derivatives of the interpolants with respect to spatial variables, which increases the accuracy and stability [193]. This feature makes it quite suitable for static and dynamic crack problems. Rabczuk and Zi [97],Rabczuk and Areias [194] proposed the extended element free Galerkin (XEFG) method for cohesive crack initiation, propagation and branching in two and three-dimensional statics and dynamics. However, the closure of the crack along the front is ensured through near-tip enrichment, which leads to the difficult selection of near-tip enrichment fields in large strain or non-linear materials. To simulate crack propagation in non-linear solids including large deformations, Zi et al. [195] proposed an XEFG method which closes the crack tip without near-tip enrichment. The entire crack is enriched by the sign function.

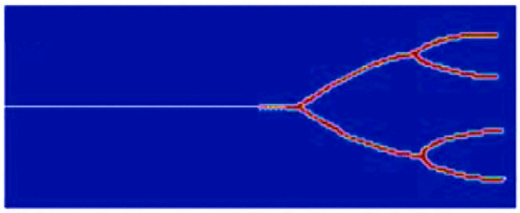

Fig. 23. A 2D example of crack branching with MMs [195].

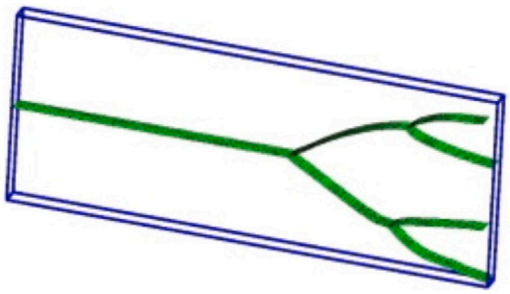

Fig. 24. A 3D example of crack branching with MMs [196].

The domain-decrease method is used to remove the branch enrichment from the discontinuous displacement field. The method is successfully applied to crack branching problems in 2D and the results agree well with the experiment results, see Fig. 23. Later, the method was extended to 3D by employing an extrinsic discontinuous enrichment and adding a Lagrange multiplier field along the crack front to close the crack by Bordas et al. [196]. In this way, the computational cost was further decreased. The method proved to be capable of modelling initiation, branching, growth and coalescence of an arbitrary number of cracks in non-linear solids by different benchmark examples. Fig. 24 shows the branching example provided in [196], which is a "2.5D" example rather than a real 3D example. The ability of the method for simulation of real 3D crack growth is demonstrated by another example of a circular–cylindrical chalk bar under torsion, which is not shown here since this example does not include the crack branching phenomenon. Rabczuk et al. [197] reviewed different crack tracking techniques in three-dimensions applicable in the context of partition of unity methods, especially meshfree methods. A crack tracking procedure is proposed and implemented in the context of XEFG and two possibilities for crack closure are presented: crack closure by crack front enrichments and crack closure without crack front enrichment by use of Lagrange multipliers. Three-dimensional crack branching examples were given and showed good agreement with the results from the literature [75].

To develop more accurate and efficient mesh-free interpolation functions, the reproducing kernel particle method (RKPM) was introduced as an improvement of the continuous SPH approximation by Liu et al. [198]. It maintains the advantages of SPH, however, because of the addition of a correction function, it gives much more accurate results. Guan et al. [199] studied the dynamic failure and fragmentation with a semi-Lagrangian RKPM, which successfully alleviated mesh distortion difficulties associated with the Lagrangian FEM. Klein et al. [200] used the virtual internal bond model with RKPM to model the propagation of cohesive cracks. The model demonstrates its capabilities of predicting the onset of crack path instabilities. With the model, simulations of crack tip instabilities and branching are conducted and theoretical analysis of branching is given.

The material point method (MPM) is a quasi-particle method introduced by Sulsky et al. [201]. In the MPM, a continuum body is described into a number of material points, which carry all the information of material properties. The material points are surrounded by a background mesh, which is used only to solve the governing equations. In each time step, the parameters and variables are transferred back and forth between material points and grids [202]. The MPM successfully eliminates the disadvantages of numerical difficulties associated with mesh distortion in Lagrangian and with the advected quantities in Eulerian description [203]. Some examples of the accurate and effective simulation of fracture propagation with MPM can be found in [204–208]. However, only one of them simulates and studies the crack branching phenomenon [208], where a phase field MPM is introduced for robust simulation of dynamic fracture in elastic media considering the anisotropic surface energy. With the model, the influence of surface energy anisotropy and loading conditions on crack patterns including crack branching are evaluated.

The MMs eliminate difficulties of mesh-based methods, such as mesh generation problems for complex 3D models, accuracy problems due to distorted or low quality meshes, adaptive remeshing resulting from dynamic problems. However, they still suffer from implementation of boundary conditions, high computational cost, instability and inconsistency problems. In addition, when modelling crack branching, crack surfaces representation and crack tracking algorithms are usually required, which introduces additional challenges associated with the numerical integration of the weak form through tracking complex crack geometry, especially for tracking complex 3D crack geometry.

4.2.2. The discontinuum methods

The peridynamics. Peridynamics (PD) is a new continuum mechanics formulation originally developed by Silling [209] in 2000. By replacing the partial differential equation with the integral equation, PD avoids the singularity and combines continuous and discontinuous descriptions together, which makes it a promising tool for the study of crack problems. There are two types of theoretical models for PD: the bond-based PD and the state-based PD. The bond-based PD assumes that any pair of particles interact only through a central potential that is totally independent of all other local conditions [78]. This assumption results in that for an isotropic, linear, microelastic material, the Poisson's ratio is limited to $1/4$ (plain strain) or $1/3$ (plane stress), which makes the bond-based PD not well suited to model complex material behaviour reliable. To remove the restrictions for Poisson's ratio, Silling et al. [210] proposed the state-based PD. In the state-based PD, the interaction between two material points depends both on the bond between the two points and the deformation of all the other bonds in the horizon. The state-based PD can be further divided into the ordinary state-based PD and non-ordinary state-based PD. Here, the bond-based PD is given as an example for simplicity to further explain the crack simulation process.

In PD, a material medium is treated as a composition of individual material points [209]. Each material point $\mathbf{x}$ is assumed to interact with the other material points $\mathbf{x}'$ around it within a local region $\mathcal{H}$, which is referred as "horizon". With a volume of V and mass density ρ, the material point is identified by its coordinates $\mathbf{x}$ in the initial configuration. The bond-based PD equation of motion at a reference position $\mathbf{x}$ and time t is given as [209]:

$$\rho(\mathbf{x})\ddot{\mathbf{u}}(\mathbf{x},t) = \int_{\mathcal{H}} \mathbf{f}(\mathbf{x}'-\mathbf{x}, \mathbf{u}'-\mathbf{u})dV + \mathbf{b}(\mathbf{x},t) \tag{19}$$

where $\mathbf{x}$ and $\mathbf{x}'$ represent the position vectors of the material point in initial configuration, $\ddot{\mathbf{u}}$ is the acceleration vector of material point $\mathbf{x}$ at time t, $\mathbf{u}$ and $\mathbf{u}'$ are the displacement of material points $\mathbf{x}$ and $\mathbf{x}'$, respectively, $\mathbf{b}$ is a prescribed body-force density field, $\mathbf{f}$ is the pairwise force defined as the force per unit volume squared between two material points $\mathbf{x}$ and $\mathbf{x}'$:

$$\mathbf{f} = cs\frac{\mathbf{y}'-\mathbf{y}}{|\mathbf{y}'-\mathbf{y}|} \tag{20}$$

in which $\mathbf{y}$ and $\mathbf{y}'$ represent the position vectors of the material point $\mathbf{x}$ and $\mathbf{x}'$ in the deformed configuration, respectively. c is the PD material parameter and is referred to as the bond-constant and the stretch s between the material points is defined as

$$s = \frac{|\mathbf{y}'-\mathbf{y}| - |\mathbf{x}'-\mathbf{x}|}{|\mathbf{x}'-\mathbf{x}|} \tag{21}$$

No complex criteria are needed during the simulation process for crack initiation and propagation as the crack growth can occur spontaneously with only one bond-break (interactions) criterion. A simple criterion for a bond-break is that if the elongation of a bond is greater than a given threshold, the bond breaks and cannot be recovered. The time taken by the bond-break is completely determined by the material geometry and loading conditions. When a series of bonds break, the discontinuous space formed by these broken bonds becomes a macroscopic crack. A variable (value between 0–1, 1 represents total failure while 0 represents no failure) is often employed to define the local damage at each point, thus, the crack path can be indicated by plotting the local damage.

Due to its intrinsic features, the PD also has the advantages of avoiding complex fracture criteria and remeshing. Applications of PD for crack branching are discussed from three perspectives in the following paragraphs.

First, by employing or improving the PD, demonstration of capturing complex crack patterns with crack branching and multiple crack branches examples is given. Ren et al. [211] proposed the dual-horizon peridynamic formulation, which naturally includes varying horizon sizes and completely solves the "ghost force" issue [212,213]. Zhou et al. [214] proposed the extended non-ordinary state-based PD, where the stress-based failure criteria are implemented. The breakage of bonds is determined by the mean stresses between the interacting material points rather than the stretch of bonds. Dipasquale et al. [215] proposed adaptive refinement algorithms for 2D peridynamic grids and as a consequence, computational resources are efficiently employed. All of the PD methods above select crack branching examples to prove their capability.

Secondly, after demonstrating the ability of capturing complex crack patterns, the PD is applied to capture various branching phenomena, including crack surface roughening, successive branching, micro-branches and multiple branches. Then numerical results from PD are compared with numerical results from other methods or results from experiments and theories. Ha and Bobaru [216] found that before branching the damage zone becomes thicker through PD simulation, which is similar to the roughening before branching observed in the experiments. Later, Ha and Bobaru [217] found that the PD model captures experimentally observed successive branching events and secondary cracking. It is found by Agwai et al. [113] that the PD simulation can capture small branches in the glass plate before the crack splits into two main branches. The micro-branches are in good agreement with experimental results. Bobaru and Zhang [218] observed that as loading increases, multiple branches are observed in soda-lime glass under stress on boundaries, see Fig. 25. From the figure, multiple branches and the widening of damage zone before branching can be observed. With a 3D PD model, Butt and Meschke [219] simulated a local crack front bifurcation grow into a micro-branch, which arrests soon or grows into a macro-branch. Distinct features on the crack surface due to the localized bifurcations and micro-branches are also captured with the model, known as "mirror", "mist" and "hackle" fracture surfaces in experimental observations [13], see Fig. 26.

Thirdly, through the observation of various phenomena, influencing factors and the mechanisms of crack branching are discussed and analysed. Ha and Bobaru [216] summarized that reflecting stress waves from the boundaries have a strong influence on the shape and structure of the crack paths in dynamic fractures. Later, Bobaru and Hu [220] explained why in the simulation of [216] the propagation velocity of a dynamic crack is influenced by the horizon size. This is because the crack propagation velocity, crack

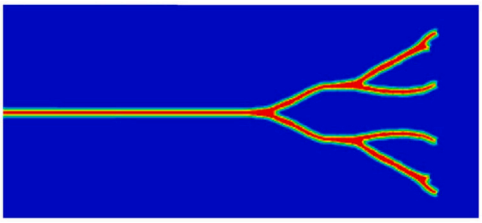

Fig. 25. A 2D example of crack branching with PD [218].

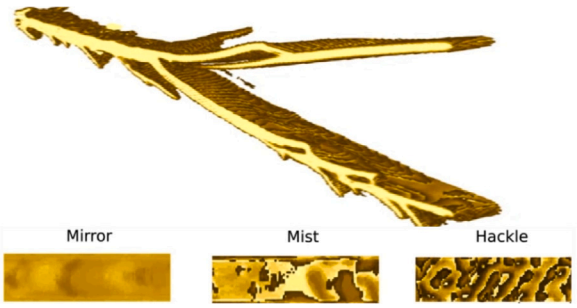

Fig. 26. A 3D example of crack branching with PD [219].

branching angles and branching time are independent of the horizon size only in the condition that the fracture process does not interact with the stress waves. Chen et al. [221] assumed that the branching moment and velocity are very sensitive to the micro-modulus function as the branching velocity after the first branching moment can slightly increase or decrease or stay constant under various micro-modulus functions. Through PD simulations under various conditions, Bobaru and Zhang [218] proposed that stress waves pile up around the crack tip and lead to "migration" of damage sufficiently large, thus the material in front of the original crack tip becomes relaxed and the crack branching ensues. Butt and Meschke [219] explained the influence of PD horizon, dimensionality and specimen size on dynamic fracture propagation with PD analysis. All of them have an influence on the crack branching patterns.

Generally speaking, the PD has been observed to perform well in modelling branching problems by circumventing difficulties in remeshing and the requirement of an external branching criterion. In addition, it has the ability of modelling multiple branches, widening of damage zone (fracture roughness) and micro-branches. However, more research is required to improve existing PD methods for better computational efficiency compared with traditional methods such as FEM. Though the remeshing process in FEM is eliminated, they introduce additional challenge associated with the numerical integration through tracking complex 3D crack geometry/surfaces. In addition, as a nonlocal method, the implementation of boundary conditions needs to be considered.

The discrete element method. Originally developed by Cundall and Strack [222], the discrete element method (DEM) has been used in the modelling of jointed structures and granular materials. It models the bulk material as discontinuum and can also be applied in modelling of fracturing and fragmentation, where the discontinuities are the natural outcome of the deformation process [223]. As a discontinuum method, the DEM treats a material medium as an assembly of distinct particles, the motion of particles is governed by Newton's laws, and forces between particles are calculated according to the small overlap between them. In DEM crack simulation, when the maximum stress exceeds the tensile or shear strength, cracks initiate and propagate [92]:

$$\begin{aligned} F_n &= k_n u_n \\ \Delta F_s &= k_s \Delta u_s \\ \frac{|F_s|}{A} &\le c_d + \frac{F_n \tan\beta}{A} \end{aligned} \tag{22}$$

where F_n is the normal force, A is the area, k_n is the normal stiffness, u_n is the normal displacement, ΔF_s is the change in shear force, k_s is the shear stiffness, Δu_s is the incremental shear displacement and c_d and β are the cohesion and joint friction angle, respectively. An example of fracture simulation using the DEM is given in Fig. 27.

DEMs can be classified with various criteria, e.g. the type of contact between bodies, the representation of deformability of solid bodies, the methodology for detection and revision of contacts, and the solution procedure for the equations of motion [225]. Though solution procedure for modelling crack propagation with DEM is different with different deformability of solid bodies (the explicit and implicit one), some steps are indispensable [223]: (1) identification of the unit (rock blocks, material particles, mechanical parts or fracture systems) system topology; (2) formulation and solution of equations of motion of the individual units; (3) the detection and updating of varying contacts (or connectivity) between the units as the consequences of their motions and deformations. The

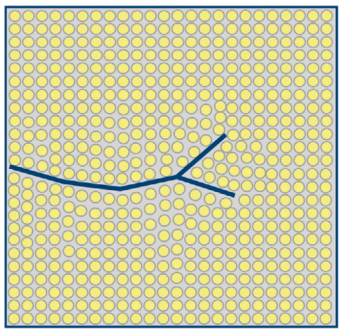

Fig. 27. A schematic illustration of crack branching with DEM.

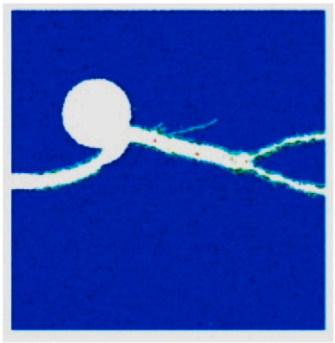

Fig. 28. A numerical example of crack branching with DEM [224].

DEM differs from other methods based on continuum mechanics e.g. FEM in that the contacts between units are varying with time and deformation while remaining fixed in other methods. The DEM is most successful in modelling granular materials. Its applications in modelling continuum materials are being explored, but have various limitations.

Due to the unique nature of DEM, it can model crack branching with taking into account heterogeneities [226]. Some examples of using DEM to study the crack branching in heterogeneous materials are listed below. Taking into account the effect of local heterogeneity around the crack tip, Hedjazi et al. [224] modelled crack branching in a vitreous biopolymer material based on DEM, see Fig. 28. A hole is set in the material to investigate the influence of the position of the hole on crack branching patterns. The results showed that DEM is more sensitive to stress heterogeneities and has better agreement with experimental results than FEM. Hofmann et al. [227] studied fracture branching with a grain-based modelling approach and found that complex fracture patterns are governed by material heterogeneity and model discretization. Chung et al. [228] used DEM to model microcracks initiation and propagation in different crystal structures, and found that the crack branching pattern varies with different notch inclination angles: the larger the notch inclination angle is, the more branching occurs.

Though DEM can be applied in the crack branching simulation in heterogeneous materials, its limitations are very obvious: (1) it is not well suited to model complex material behaviour reliably and its application is mostly limited to granular materials; (2) it is awkward in predicting a variety of macroscopic properties (e.g. elastic stiffness, strength, critical energy release rate for uni-, bi- and tri-axial loading, etc.); (3) it usually has high computational cost, which is easily influenced by many factors, such as particle numbers, particle shapes and contact force models [223].

5. Summary and prospective work

This paper presents an overview of crack branching, including experimental observations, physics of crack branching, and crack models and numerical methods for simulation of crack branching problems. In terms of experimental observations, high speed photography is the most commonly used technique to be combined with photoelasticity, caustics, digital image correlation, digital gradient sensing to study the crack branching. The current focus is on (1) how to combine and improve upon existing shortcomings with the combination of technology development; (2) how to simplify the operations and reduce operating costs while ensuring high temporal and spatial resolution. Supported by experimental research, physics of branching including the causes of crack branching and branching criteria have been investigated and summarized. One explanation suggests the branching occurs once the crack velocity exceeds a critical value (related to the wave speed). Another explanation assumes branching is a natural outcome of the growth of microcracks near the crack tip and energy absorbed into the crack is related to the limiting velocity. Dynamic instabilities, which are related to critical velocity, fracture roughness and micro-branches, are also shown to be a strong mechanism for crack

branching and are investigated. In addition, the crack front waves and the tilting and twisting of the stress vector at the crack front are responsible for the crack branching. Corresponding to these potential causes to crack branching, different branching criteria have been proposed, including external and internal criteria. The crack models and numerical methods for crack branching have been developed and continuously improved according to various crack branching criteria, which are further applied to simulate crack branching, to shed light on the mechanisms behind branching. These models and methods are reviewed in this paper with respect to their strengths and limitations.

Several outstanding issues and challenges are identified and need to be resolved for reliable crack branching prediction, these include the limitation of experimental techniques for the observation and measurements of physical parameters in front of the crack tip; current analytical techniques and existing branching criteria are not sufficient to define the mechanisms driving crack branching and associated dynamic instabilities; the limitations of various crack models and numerical methods proposed for simulating complex fracture propagation processes. Moreover, the study of the branching problem is further complicated by considerations such as heterogeneity of the material, softening behaviour and large fracture networks in which multiple length scale cracks develop.

Declaration of competing interest

The authors declare that they have no known competing financial interests or personal relationships that could have appeared to influence the work reported in this paper.

Acknowledgements

The authors would like to thank the supports from China Scholarship Council (CSC No.: 201709370055), Swansea University (Zienkiewicz Scholarship), and the Royal Society (Ref.: IEC\NSFC\191628).

References

[1] Kalthoff J. On the propagation direction of bifurcated cracks. In: Proceedings of an international conference on dynamic crack propagation. Springer; 1973, p. 449–58.
[2] Nishioka T, Furutuka J, Tchouikov S, Fujimoto T. Generation-phase simulation of dynamic crack bifurcation phenomenon using moving finite element method based on delaunay automatic triangulation. Comput Model Eng Sci 2002;3(1):129–45.
[3] Anderson TL. Fracture mechanics: Fundamentals and applications. CRC Press; 2017.
[4] Ramulu M, Kobayashi A. Mechanics of crack curving and branching—a dynamic fracture analysis. Dyn Fract 1985;61–75.
[5] Guozden TM, Jagla EA, Marder M. Supersonic cracks in lattice models. Int J Fract 2010;162(1–2):107–25.
[6] Freund L. Dynamic fracture mechanics. Cambridge monographs on mechanics, Cambridge University Press; 1998.
[7] Ravi-Chandar K. Dynamic fracture. Elsevier Science; 2004.
[8] Schardin H. Velocity effects in fracture. In: ICF0, Swampscott-MA (USA) 1959. 1959, p. 297–330.
[9] Kerkhof F. General lecture wave fractographic investigations of brittle fracture dynamics. In: Proceedings of an international conference on dynamic crack propagation. Springer; 1973, p. 3–35.
[10] Kobayashi A, Mall S. Dynamic fracture toughness of Homalite-100. Exp Mech 1978;18(1):11–8.
[11] Dally JW. Dynamic photoelastic studies of fracture. Exp Mech 1979;19(10):349–61.
[12] Ravi-Chandar K, Knauss W. An experimental investigation into dynamic fracture: I. Crack initiation and arrest. Int J Fract 1984;25(4):247–62.
[13] Ravi-Chandar K, Knauss W. An experimental investigation into dynamic fracture: II. Microstructural aspects. Int J Fract 1984;26(1):65–80.
[14] Ravi-Chandar K, Knauss W. An experimental investigation into dynamic fracture: III. On steady-state crack propagation and crack branching. Int J Fract 1984;26(2):141–54.
[15] Ravi-Chandar K, Knauss W. An experimental investigation into dynamic fracture: IV. On the interaction of stress waves with propagating cracks. Int J Fract 1984;26(3):189–200.
[16] Fineberg J, Gross SP, Marder M, Swinney HL. Instability in dynamic fracture. Phys Rev Lett 1991;67(4):457.
[17] Fineberg J, Gross SP, Marder M, Swinney HL. Instability in the propagation of fast cracks. Phys Rev B 1992;45(10):5146.
[18] Sharon E, Gross SP, Fineberg J. Local crack branching as a mechanism for instability in dynamic fracture. Phys Rev Lett 1995;74(25):5096.
[19] Sharon E, Fineberg J. Microbranching instability and the dynamic fracture of brittle materials. Phys Rev B 1996;54(10):7128.
[20] Sharon E, Gross SP, Fineberg J. Energy dissipation in dynamic fracture. Phys Rev Lett 1996;76(12):2117.
[21] Fineberg J, Marder M. Instability in dynamic fracture. Phys Rep 1999;313(1–2):1–108.
[22] Bouchbinder E, Livne A, Fineberg J. Weakly nonlinear theory of dynamic fracture. Phys Rev Lett 2008;101(26):264302.
[23] Bouchbinder E, Livne A, Fineberg J. Weakly nonlinear fracture mechanics: experiments and theory. Int J Fract 2010;162(1–2):3–20.
[24] Bouchbinder E, Goldman T, Fineberg J. The dynamics of rapid fracture: instabilities, nonlinearities and length scales. Rep Progr Phys 2014;77(4):046501.
[25] Livne A, Ben-David O, Fineberg J. Oscillations in rapid fracture. Phys Rev Lett 2007;98(12):124301.
[26] Fineberg J, Bouchbinder E. Recent developments in dynamic fracture: some perspectives. Int J Fract 2015;196(1–2):33–57.
[27] Hawong J, Kobayashi A, Dadkhah M, Kang B-J, Ramulu M. Dynamic crack curving and branching under biaxial loading. Exp Mech 1987;27(2):146–53.
[28] Hauch J, Marder M. Energy balance in dynamic fracture, investigated by a potential drop technique. Int J Fract 1998;90(1–2):133–51.
[29] Suzuki S, Sakaue K, Iwanaga K. Measurement of energy release rate and energy flux of rapidly bifurcating crack in Homalite 100 and Araldite B by high-speed holographic microscopy. J Mech Phys Solids 2007;55(7):1487–512.
[30] Murphy N, Ali M, Ivankovic A. Dynamic crack bifurcation in PMMA. Eng Fract Mech 2006;73(16):2569–87.
[31] Fayyad TM, Lees JM. Experimental investigation of crack propagation and crack branching in lightly reinforced concrete beams using digital image correlation. Eng Fract Mech 2017;182:487–505.
[32] Skarżyński Ł, Tejchman J. Experimental investigations of fracture process using DIC in plain and reinforced concrete beams under bending. Strain 2013;49(6):521–43.
[33] Sundaram BM, Tippur HV. Dynamic fracture of soda-lime glass: A full-field optical investigation of crack initiation, propagation and branching. J Mech Phys Solids 2018;120:132–53.
[34] Bleyer J, Roux-Langlois C, Molinari J-F. Dynamic crack propagation with a variational phase-field model: limiting speed, crack branching and velocity-toughening mechanisms. Int J Fract 2017;204(1):79–100.

[35] Dempsey JP. Dynamic crack division in brittle solids. In: Twelfth canadian congress of applied mechanics. 1989, p. 200–1.
[36] Kobayashi A, Ramulu M. A dynamic fracture analysis of crack curving and branching. Le J Phys Colloques 1985;46(C5):C5–197.
[37] Kobayashi A. Handbook on experimental mechanics. Englewood Cliffs, NJ: Prentice-Hall, Inc., 1987, 1020; 1987.
[38] Suzuki S, Sakaue K. Measurement of crack opening displacement and energy release rate of rapidly bifurcating cracks in PMMA by high-speed holographic microscopy. JSME Int J Ser A Solid Mech Mater Eng 2004;47(3):264–73.
[39] Hull D. Fractography: Observing, measuring and interpreting fracture surface topography. Cambridge University Press; 1999.
[40] Ivankovic A, Pandya K, Williams J. Crack growth predictions in polyethylene using measured traction–separation curves. Eng Fract Mech 2004;71(4–6):657–68.
[41] Yoffe EH. LXXV. The moving griffith crack. Lond Edinb Dubl Philos Mag J Sci 1951;42(330):739–50.
[42] Broberg KB. The propagation of a brittle crack. Arkvik Fysik 1960;18:159–92.
[43] Eshelby J. Inelastic behavior of solids. Ed Kanninen 1970;77–115.
[44] Gao H. Surface roughening and branching instabilities in dynamic fracture. J Mech Phys Solids 1993;41(3):457–86.
[45] Livne A, Cohen G, Fineberg J. Universality and hysteretic dynamics in rapid fracture. Phys Rev Lett 2005;94(22):224301.
[46] Adda-Bedia M, Arias R. Brittle fracture dynamics with arbitrary paths I. Kinking of a dynamic crack in general antiplane loading. J Mech Phys Solids 2003;51(7):1287–304.
[47] Adda-Bedia M. Brittle fracture dynamics with arbitrary paths. II. Dynamic crack branching under general antiplane loading. J Mech Phys Solids 2004;52(6):1407–20.
[48] Adda-Bedia M. Brittle fracture dynamics with arbitrary paths III. The branching instability under general loading. J Mech Phys Solids 2005;53(1):227–48.
[49] Katzav E, Adda-Bedia M, Arias R. Theory of dynamic crack branching in brittle materials. Int J Fract 2007;143(3):245–71.
[50] Adda-Bedia M, Arias RE, Bouchbinder E, Katzav E. Dynamic stability of crack fronts: out-of-plane corrugations. Phys Rev Lett 2013;110(1):014302.
[51] Sharon E, Cohen G, Fineberg J. Crack front waves and the dynamics of a rapidly moving crack. Phys Rev Lett 2002;88(8):085503.
[52] Bonamy D, Ravi-Chandar K. Dynamic crack response to a localized shear pulse perturbation in brittle amorphous materials: on crack surface roughening. Int J Fract 2005;134(1):1–22.
[53] Buehler MJ, Abraham FF, Gao H. Hyperelasticity governs dynamic fracture at a critical length scale. Nature 2003;426(6963):141–6.
[54] Abraham FF, Gao H. How fast can cracks propagate? Phys Rev Lett 2000;84(14):3113.
[55] Gross SP, Fineberg J, Marder M, McCormick W, Swinney HL. Acoustic emissions from rapidly moving cracks. Phys Rev Lett 1993;71(19):3162.
[56] Linder C, Armero F. Finite elements with embedded branching. Finite Elem Anal Des 2009;45(4):280–93.
[57] Armero F, Linder C. Numerical simulation of dynamic fracture using finite elements with embedded discontinuities. Int J Fract 2009;160(2):119.
[58] Xu D, Liu Z, Liu X, Zeng Q, Zhuang Z. Modelling of dynamic crack branching by enhanced extended finite element method. Comput Mech 2014;54(2):489–502.
[59] Freund L. Crack propagation in an elastic solid subjected to general loading—I. constant rate of extension. J Mech Phys Solids 1972;20(3):129–40.
[60] Freund L. Crack propagation in an elastic solid subjected to general loading—II. Non-uniform rate of extension. J Mech Phys Solids 1972;20(3):141–52.
[61] Freund L. Crack propagation in an elastic solid subjected to general loading—III. Stress wave loading. J Mech Phys Solids 1973;21(2):47–61.
[62] Clark A, Irwin G. Crack-propagation behaviors. Exp Mech 1966;6(6):321–30.
[63] Kishen JC, Singh KD. Stress intensity factors based fracture criteria for kinking and branching of interface crack: application to dams. Eng Fract Mech 2001;68(2):201–19.
[64] Rafiee S, Seelig T, Gross D. Simulation of dynamic crack curving and branching under biaxial loading by a time domain boundary integral equation method. Int J Fract 2003;120(3):545–61.
[65] Zehnder A. Fracture mechanics. Lecture notes in applied and computational mechanics, Springer Netherlands; 2012, URL https://books.google.co.uk/booksid=714J5kXbYocC.
[66] Tchouikov S, Nishioka T, Fujimoto T. Numerical prediction of dynamically propagating and branching cracks using moving finite element method. CMC: Comput Mater Contin 2004;1(2):191–204.
[67] Xie Y, Hu X, Wang X, Chen J, Lee K. A theoretical note on mode-I crack branching and kinking. Eng Fract Mech 2011;78(6):919–29.
[68] Dempsey J, Kuo M-K, Achenbach JD. Mode-III crack kinking under stress-wave loading. Wave Motion 1982;4(2):181–90.
[69] Burgers P. Dynamic propagation of a kinked or bifurcated crack in antiplane strain. J Appl Mech 1982;49:371.
[70] Burgers P. Dynamic kinking of a crack in plane strain. Int J Solids Struct 1983;19(8):735–52.
[71] Griffith AA. VI. The phenomena of rupture and flow in solids. Philos Trans R Soc Lond Ser A 1921;221(582–593):163–98.
[72] Gol'dstein RV, Salganik RL. Brittle fracture of solids with arbitrary cracks. Int J Fract 1974;10(4):507–23.
[73] Xu X-P, Needleman A. Numerical simulations of fast crack growth in brittle solids. J Mech Phys Solids 1994;42(9):1397–434.
[74] Camacho GT, Ortiz M. Computational modelling of impact damage in brittle materials. Int J Solids Struct 1996;33(20–22):2899–938.
[75] Rabczuk T, Belytschko T. Cracking particles: a simplified meshfree method for arbitrary evolving cracks. Internat J Numer Methods Engrg 2004;61(13):2316–43.
[76] Rabczuk T, Belytschko T. A three-dimensional large deformation meshfree method for arbitrary evolving cracks. Comput Methods Appl Mech Engrg 2007;196(29–30):2777–99.
[77] Rabczuk T, Zi G, Bordas S, Nguyen-Xuan H. A simple and robust three-dimensional cracking-particle method without enrichment. Comput Methods Appl Mech Engrg 2010;199(37–40):2437–55.
[78] Madenci E, Oterkus E. Peridynamic theory. In: Peridynamic theory and its applications. Springer; 2014, p. 19–43.
[79] De Borst R. Numerical aspects of cohesive-zone models. Eng Fract Mech 2003;70(14):1743–57.
[80] de Borst R, Remmers JJ, Needleman A. Mesh-independent discrete numerical representations of cohesive-zone models. Eng Fract Mech 2006;73(2):160–77.
[81] Song J-H, Wang H, Belytschko T. A comparative study on finite element methods for dynamic fracture. Comput Mech 2008;42(2):239–50.
[82] Pandolfi A, Ortiz M. An eigenerosion approach to brittle fracture. Internat J Numer Methods Engrg 2012;92(8):694–714.
[83] Stochino F, Qinami A, Kaliske M. Eigenerosion for static and dynamic brittle fracture. Eng Fract Mech 2017;182:537–51.
[84] Belytschko T, Black T. Elastic crack growth in finite elements with minimal remeshing. Internat J Numer Methods Engrg 1999;45(5):601–20.
[85] Moës N, Dolbow J, Belytschko T. A finite element method for crack growth without remeshing. Internat J Numer Methods Engrg 1999;46(1):131–50.
[86] Rabczuk T, Song J-H, Zhuang X, Anitescu C. Extended finite element and meshfree methods. Academic Press; 2019.
[87] Bourdin B, Francfort GA, Marigo J-J. Numerical experiments in revisited brittle fracture. J Mech Phys Solids 2000;48(4):797–826.
[88] Borden MJ, Verhoosel CV, Scott MA, Hughes TJ, Landis CM. A phase-field description of dynamic brittle fracture. Comput Methods Appl Mech Engrg 2012;217:77–95.
[89] Bažant ZP, Jirásek M. Nonlocal integral formulations of plasticity and damage: survey of progress. J Eng Mech 2002;128(11):1119–49.
[90] Friedman J, Popescu BE. Gradient directed regularization for linear regression and classification. Technical report, Statistics Department, Stanford University; 2003.
[91] Rabczuk T. Computational methods for fracture in brittle and quasi-brittle solids: state-of-the-art review and future perspectives. ISRN Appl Math 2013;2013.
[92] Mohammadnejad M, Liu H, Chan A, Dehkhoda S, Fukuda D. An overview on advances in computational fracture mechanics of rock. Geosyst Eng 2018;1–24.

[93] Jung J, Yang Q. A two-dimensional augmented finite element for dynamic crack initiation and propagation. Int J Fract 2017;203(1–2):41–61.
[94] Schmidt B, Fraternali F, Ortiz M. Eigenfracture: an eigendeformation approach to variational fracture. Multiscale Model Simul 2009;7(3):1237–66.
[95] Fan Z, Liao H, Jiang H, Wang H, Li B. A dynamic adaptive eigenfracture method for failure in brittle materials. Eng Fract Mech 2021;244:107540.
[96] Fries T-P, Belytschko T. The extended/generalized finite element method: an overview of the method and its applications. Internat J Numer Methods Engrg 2010;84(3):253–304.
[97] Rabczuk T, Zi G. A meshfree method based on the local partition of unity for cohesive cracks. Comput Mech 2007;39(6):743–60.
[98] Rabczuk T, Song J-H, Belytschko T. Simulations of instability in dynamic fracture by the cracking particles method. Eng Fract Mech 2009;76(6):730–41.
[99] Ai W, Augarde CE. An adaptive cracking particle method for 2D crack propagation. Internat J Numer Methods Engrg 2016;108(13):1626–48.
[100] Ai W, Augarde CE. A multi-cracked particle method for complex fracture problems in 2D. Math Comput Simulation 2018;150:1–24.
[101] Xu S. Stable cracking particles method based on stabilized nodal integration and updated Lagrangian kernel. Math Probl Eng 2014;2014.
[102] Dugdale DS. Yielding of steel sheets containing slits. J Mech Phys Solids 1960;8(2):100–4.
[103] Barenblatt GI. The mathematical theory of equilibrium cracks in brittle fracture. Advances in applied mechanics, vol. 7, Elsevier; 1962, p. 55–129.
[104] Needleman A. A continuum model for void nucleation by inclusion debonding. J Appl Mech 1987;54(3):525–31.
[105] Geubelle PH, Baylor JS. Impact-induced delamination of composites: a 2D simulation. Composites B 1998;29(5):589–602.
[106] Pandolfi A, Ortiz M. An efficient adaptive procedure for three-dimensional fragmentation simulations. Eng Comput 2002;18(2):148–59.
[107] Park K, Paulino GH. Cohesive zone models: a critical review of traction-separation relationships across fracture surfaces. Appl Mech Rev 2011;64(6).
[108] Seagraves A, Radovitzky R. Advances in cohesive zone modeling of dynamic fracture. In: Dynamic failure of materials and structures. Springer; 2009, p. 349–405.
[109] Papoulia KD, Sam C-H, Vavasis SA. Time continuity in cohesive finite element modelling. Internat J Numer Methods Engrg 2003;58(5):679–701.
[110] Radovitzky R, Seagraves A, Tupek M, Noels L. A scalable 3D fracture and fragmentation algorithm based on a hybrid, discontinuous Galerkin, cohesive element method. Comput Methods Appl Mech Engrg 2011;200(1–4):326–44.
[111] Sam C-H, Papoulia KD, Vavasis SA. Obtaining initially rigid cohesive finite element models that are temporally convergent. Eng Fract Mech 2005;72(14):2247–67.
[112] Arias I, Knap J, Chalivendra VB, Hong S, Ortiz M, Rosakis AJ. Numerical modelling and experimental validation of dynamic fracture events along weak planes. Comput Methods Appl Mech Engrg 2007;196(37–40):3833–40.
[113] Agwai A, Guven I, Madenci E. Predicting crack propagation with peridynamics: a comparative study. Int J Fract 2011;171(1):65.
[114] Paulino GH, Park K, Celes W, Espinha R. Adaptive dynamic cohesive fracture simulation using nodal perturbation and edge-swap operators. Internat J Numer Methods Engrg 2010;84(11):1303–43.
[115] Leon S, Spring D, Paulino G. Reduction in mesh bias for dynamic fracture using adaptive splitting of polygonal finite elements. Internat J Numer Methods Engrg 2014;100(8):555–76.
[116] Spring DW, Leon SE, Paulino GH. Unstructured polygonal meshes with adaptive refinement for the numerical simulation of dynamic cohesive fracture. Int J Fract 2014;189(1):33–57.
[117] Choi H, Park K. Removing mesh bias in mixed-mode cohesive fracture simulation with stress recovery and domain integral. Internat J Numer Methods Engrg 2019;120(9):1047–70.
[118] Zhang Z, Paulino GH, Celes W. Extrinsic cohesive modelling of dynamic fracture and microbranching instability in brittle materials. Internat J Numer Methods Engrg 2007;72(8):893–923.
[119] Miller O, Freund L, Needleman A. Energy dissipation in dynamic fracture of brittle materials. Modelling Simulation Mater Sci Eng 1999;7(4):573.
[120] Park K, Paulino GH, Celes W, Espinha R. Adaptive mesh refinement and coarsening for cohesive zone modelling of dynamic fracture. Internat J Numer Methods Engrg 2012;92(1):1–35.
[121] Nguyen VP. Discontinuous Galerkin/extrinsic cohesive zone modelling: Implementation caveats and applications in computational fracture mechanics. Eng Fract Mech 2014;128:37–68.
[122] Becker G, Noels L. A full-discontinuous Galerkin formulation of nonlinear Kirchhoff–Love shells: elasto-plastic finite deformations, parallel computation, and fracture applications. Internat J Numer Methods Engrg 2013;93(1):80–117.
[123] Baek H, Kweon C, Park K. Multiscale dynamic fracture analysis of composite materials using adaptive microstructure modeling. Internat J Numer Methods Engrg 2020;121(24):5719–41.
[124] Park K, Paulino GH, Roesler JR. A unified potential-based cohesive model of mixed-mode fracture. J Mech Phys Solids 2009;57(6):891–908.
[125] Park K, Paulino GH. Computational implementation of the PPR potential-based cohesive model in ABAQUS: Educational perspective. Eng Fract Mech 2012;93:239–62.
[126] Park K, Choi H, Paulino GH. Assessment of cohesive traction-separation relationships in ABAQUS: A comparative study. Mech Res Commun 2016;78:71–8.
[127] Baek H, Park K. Cohesive frictional-contact model for dynamic fracture simulations under compression. Int J Solids Struct 2018;144:86–99.
[128] Abedi R, Haber RB, Clarke PL. Effect of random defects on dynamic fracture in quasi-brittle materials. Int J Fract 2017;208(1):241–68.
[129] Francfort GA, Marigo J-J. Revisiting brittle fracture as an energy minimization problem. J Mech Phys Solids 1998;46(8):1319–42.
[130] Chen B, Sun Y, Barboza BR, Barron AR, Li C. Phase-field simulation of hydraulic fracturing with a revised fluid model and hybrid solver. Eng Fract Mech 2020;229:106928.
[131] Hofacker M, Miehe C. Continuum phase field modeling of dynamic fracture: variational principles and staggered FE implementation. Int J Fract 2012;178(1–2):113–29.
[132] Bleyer J, Molinari J-F. Microbranching instability in phase-field modelling of dynamic brittle fracture. Appl Phys Lett 2017;110(15):151903.
[133] Wu J-Y, Nguyen VP. A length scale insensitive phase-field damage model for brittle fracture. J Mech Phys Solids 2018;119:20–42.
[134] Wu J-Y. A unified phase-field theory for the mechanics of damage and quasi-brittle failure. J Mech Phys Solids 2017;103:72–99.
[135] Nguyen VP, Wu J-Y. Modeling dynamic fracture of solids with a phase-field regularized cohesive zone model. Comput Methods Appl Mech Engrg 2018;340:1000–22.
[136] Zhou S, Zhuang X, Zhu H, Rabczuk T. Phase field modelling of crack propagation, branching and coalescence in rocks. Theor Appl Fract Mech 2018;96:174–92.
[137] Zhou S, Zhuang X, Rabczuk T. Phase-field modelling of fluid-driven dynamic cracking in porous media. Comput Methods Appl Mech Engrg 2019.
[138] Ren H, Zhuang X, Anitescu C, Rabczuk T. An explicit phase field method for brittle dynamic fracture. Comput Struct 2019;217:45–56.
[139] Wu J-Y, Nguyen VP, Nguyen CT, Sutula D, Bordas S, Sinaie S. Phase field modeling of fracture. Adv Appl Mech: Multi-Scale Theory Comput 2018;52.
[140] Hofacker M, Miehe C. A phase field model of dynamic fracture: Robust field updates for the analysis of complex crack patterns. Internat J Numer Methods Engrg 2013;93(3):276–301.
[141] Henry H. Study of the branching instability using a phase field model of inplane crack propagation. Europhys Lett 2008;83(1):16004.
[142] Tian F, Tang X, Xu T, Yang J, Li L. Bifurcation criterion and the origin of limit crack velocity in dynamic brittle fracture. Int J Fract 2020;224:117–31.
[143] Mandal TK, Nguyen VP, Wu J-Y. Evaluation of variational phase-field models for dynamic brittle fracture. Eng Fract Mech 2020;235:107169.
[144] Dinachandra M, Alankar A. A phase-field study of crack propagation and branching in functionally graded materials using explicit dynamics. Theor Appl Fract Mech 2020;109:102681.
[145] Kamensky D, Moutsanidis G, Bazilevs Y. Hyperbolic phase field modeling of brittle fracture: part I—theory and simulations. J Mech Phys Solids 2018;121:81–98.

[146] Liu G, Li Q, Msekh MA, Zuo Z. Abaqus implementation of monolithic and staggered schemes for quasi-static and dynamic fracture phase-field model. Comput Mater Sci 2016;121:35–47.
[147] Zhou S, Rabczuk T, Zhuang X. Phase field modeling of quasi-static and dynamic crack propagation: COMSOL implementation and case studies. Adv Eng Softw 2018;122:31–49.
[148] Steinke C, Özenç K, Chinaryan G, Kaliske M. A comparative study of the r-adaptive material force approach and the phase-field method in dynamic fracture. Int J Fract 2016;201(1):97–118.
[149] Jirasek M. Nonlocal models for damage and fracture: comparison of approaches. Int J Solids Struct 1998;35(31–32):4133–45.
[150] Karihaloo B. Failure of concrete. In: Milne I, Ritchie R, Karihaloo B, editors. Comprehensive structural integrity. Oxford: Pergamon; 2003, p. 477–548. http://dx.doi.org/10.1016/B0-08-043749-4/02087-5.
[151] Wolff C, Richart N, Molinari J-F. A non-local continuum damage approach to model dynamic crack branching. Internat J Numer Methods Engrg 2015;101(12):933–49.
[152] Wang Z, Shedbale AS, Kumar S, Poh LH. Localizing gradient damage model with micro inertia effect for dynamic fracture. Comput Methods Appl Mech Engrg 2019;355:492–512.
[153] Milne I, Ritchie RO, Karihaloo BL. Comprehensive structural integrity: cyclic loading and fatigue, vol. 4. Elsevier; 2003.
[154] Pradhan KK, Chakraverty S. Chapter four - finite element method. In: Pradhan KK, Chakraverty S, editors. Computational structural mechanics. Academic Press; 2019, p. 25–8. http://dx.doi.org/10.1016/B978-0-12-815492-2.00010-1.
[155] Chen B, Cen S, Barron AR, Owen D, Li C. Numerical investigation of the fluid lag during hydraulic fracturing. Eng Comput 2018;35(5):2050–77.
[156] Newmark NM. A method of computation for structural dynamics. J Eng Mech Div 1959;85(3):67–94.
[157] Zhuang Z, Liu Z, Cheng B, Liao J. Extended finite element method. Tsinghua University Press computational mechanics, Elsevier Science; 2014.
[158] Gupta V, Duarte CA, Babuška I, Banerjee U. A stable and optimally convergent generalized FEM (SGFEM) for linear elastic fracture mechanics. Comput Methods Appl Mech Engrg 2013;266:23–39.
[159] Gupta V, Duarte C, Babuška I, Banerjee U. Stable GFEM (SGFEM): Improved conditioning and accuracy of GFEM/XFEM for three-dimensional fracture mechanics. Comput Methods Appl Mech Engrg 2015;289:355–86.
[160] Wu J-Y, Li F-B. An improved stable XFEM (Is-XFEM) with a novel enrichment function for the computational modeling of cohesive cracks. Comput Methods Appl Mech Engrg 2015;295:77–107.
[161] Khoei A. Extended finite element method: theory and applications. Wiley series in computational mechanics, Wiley; 2015, URL https://books.google.co.uk/books?id=unKwCQAAQBAJ.
[162] Daux C, Moës N, Dolbow J, Sukumar N, Belytschko T. Arbitrary branched and intersecting cracks with the extended finite element method. Internat J Numer Methods Engrg 2000;48(12):1741–60.
[163] Belytschko T, Chen H, Xu J, Zi G. Dynamic crack propagation based on loss of hyperbolicity and a new discontinuous enrichment. Internat J Numer Methods Engrg 2003;58(12):1873–905.
[164] Chen J-W, Zhou X-P. The enhanced extended finite element method for the propagation of complex branched cracks. Eng Anal Bound Elem 2019;104:46–62.
[165] Song J-H, Areias PM, Belytschko T. A method for dynamic crack and shear band propagation with phantom nodes. Internat J Numer Methods Engrg 2006;67(6):868–93.
[166] Song J-H, Belytschko T. Cracking node method for dynamic fracture with finite elements. Internat J Numer Methods Engrg 2009;77(3):360–85.
[167] Aliabadi MH. Boundary element methods in linear elastic fracture mechanics. In: Reference module in materials science and materials engineering. Elsevier; 2016.
[168] Liu Y, Mukherjee S, Nishimura N, Schanz M, Ye W, Sutradhar A, Pan E, Dumont NA, Frangi A, Saez A. Recent advances and emerging applications of the boundary element method. Appl Mech Rev 2011;64(3).
[169] Seelig T, Gross D. On the interaction and branching of fast running cracks—a numerical investigation. J Mech Phys Solids 1999;47(4):935–52.
[170] Rajapakse R, Xu X-L. Boundary element modelling of cracks in piezoelectric solids. Eng Anal Bound Elem 2001;25(9):771–81.
[171] Yan X. Numerical analysis of a few complex crack problems with a boundary element method. Eng Fail Anal 2006;13(5):805–25.
[172] Marji MF. Numerical analysis of quasi-static crack branching in brittle solids by a modified displacement discontinuity method. Int J Solids Struct 2014;51(9):1716–36.
[173] Santana E, Portela A. Dual boundary element analysis of fatigue crack growth, interaction and linkup. Eng Anal Bound Elem 2016;64:176–95.
[174] Fedelinski P. Dynamically loaded branched and intersecting cracks. 2017, Czasopismo Inzynierii Ladowej, Srodowiska I Architektury.
[175] Shrivastava K, Sharma MM, et al. Mechanisms for the formation of complex fracture networks in naturally fractured rocks. In: SPE hydraulic fracturing technology conference and exhibition. Society of Petroleum Engineers; 2018.
[176] Nguyen VP, Rabczuk T, Bordas S, Duflot M. Meshless methods: a review and computer implementation aspects. Math Comput Simulation 2008;79(3):763–813.
[177] Wang H, Qin Q-H. Methods of fundamental solutions in solid mechanics. Elsevier; 2019.
[178] Gingold RA, Monaghan JJ. Smoothed particle hydrodynamics: theory and application to non-spherical stars. Mon Not R Astron Soc 1977;181(3):375–89.
[179] Liu G-R, Gu Y-T. An introduction to meshfree methods and their programming. Springer Science & Business Media; 2005.
[180] Zhuang X, Augarde C, Mathisen K. Fracture modeling using meshless methods and level sets in 3D: framework and modeling. Internat J Numer Methods Engrg 2012;92(11):969–98.
[181] Huerta A, Belytschko T, Fernández-Méndez S, Rabczuk T, Zhuang X, Arroyo M. Meshfree methods. In: Encyclopedia of computational mechanics. 2nd ed.. Wiley Online Library; 2018, p. 1–38.
[182] Monaghan JJ, Gingold RA. Shock simulation by the particle method SPH. J Comput Phys 1983;52(2):374–89.
[183] Libersky LD, Petschek AG, Carney TC, Hipp JR, Allahdadi FA. High strain Lagrangian hydrodynamics: a three-dimensional SPH code for dynamic material response. J Comput Phys 1993;109(1):67–75.
[184] Libersky LD, Randles PW, Carney TC, Dickinson DL. Recent improvements in SPH modeling of hypervelocity impact. Int J Impact Eng 1997;20(6–10):525–32.
[185] Randles P, Libersky LD. Smoothed particle hydrodynamics: some recent improvements and applications. Comput Methods Appl Mech Engrg 1996;139(1–4):375–408.
[186] Rabczuk T, Eibl J. Simulation of high velocity concrete fragmentation using SPH/MLSPH. Internat J Numer Methods Engrg 2003;56(10):1421–44.
[187] Rabczuk T, Eibl J. Modelling dynamic failure of concrete with meshfree methods. Int J Impact Eng 2006;32(11):1878–97.
[188] Rajagopal S, Gupta N. Meshfree modelling of fracture—a comparative study of different methods. Meccanica 2011;46(5):1145–58.
[189] Rabczuk T, Belytschko T, Xiao S. Stable particle methods based on Lagrangian kernels. Comput Methods Appl Mech Engrg 2004;193(12–14):1035–63.
[190] Vignjevic R, Reveles JR, Campbell J. SPH in a total Lagrangian formalism. CMC-Tech Science Press- 2006;4(3):181.
[191] Chakraborty S, Shaw A. A pseudo-spring based fracture model for SPH simulation of impact dynamics. Int J Impact Eng 2013;58:84–95.
[192] Islam MRI, Shaw A. Numerical modelling of crack initiation, propagation and branching under dynamic loading. Eng Fract Mech 2020;224:106760.
[193] Belytschko T, Lu YY, Gu L. Element-free Galerkin methods. Internat J Numer Methods Engrg 1994;37(2):229–56.
[194] Rabczuk T, Areias P. A meshfree thin shell for arbitrary evolving cracks based on an extrinsic basis. Comput Mech 2006.
[195] Zi G, Rabczuk T, Wall W. Extended meshfree methods without branch enrichment for cohesive cracks. Comput Mech 2007;40(2):367–82.

[196] Bordas S, Rabczuk T, Zi G. Three-dimensional crack initiation, propagation, branching and junction in non-linear materials by an extended meshfree method without asymptotic enrichment. Eng Fract Mech 2008;75(5):943–60.
[197] Rabczuk T, Bordas S, Zi G. On three-dimensional modelling of crack growth using partition of unity methods. Comput Struct 2010;88(23–24):1391–411.
[198] Liu WK, Jun S, Zhang YF. Reproducing kernel particle methods. Internat J Numer Methods Fluids 1995;20(8–9):1081–106.
[199] Guan P-C, Chi S, Chen J, Slawson T, Roth M. Semi-Lagrangian reproducing kernel particle method for fragment-impact problems. Int J Impact Eng 2011;38(12):1033–47.
[200] Klein P, Foulk J, Chen E, Wimmer S, Gao H. Physics-based modelling of brittle fracture: cohesive formulations and the application of meshfree methods. Theor Appl Fract Mech 2001;37(1–3):99–166.
[201] Sulsky D, Chen Z, Schreyer HL. A particle method for history-dependent materials. Comput Methods Appl Mech Engrg 1994;118(1–2):179–96.
[202] Li S, Zhang Y, Wu J, Yu J, Gong X. Modeling of crack propagation with the quasi-static material point method. Eng Fract Mech 2021;245:107602.
[203] Ma S, Zhang X. Material point method for impact and explosion problems. In: Computational mechanics. Springer; 2007, p. 156–66.
[204] Schreyer H, Sulsky D, Zhou S-J. Modeling delamination as a strong discontinuity with the material point method. Comput Methods Appl Mech Engrg 2002;191(23–24):2483–507.
[205] Nairn JA. Material point method calculations with explicit cracks. Comput Model Eng Sci 2003;4(6):649–64.
[206] Liang Y, Benedek T, Zhang X, Liu Y. Material point method with enriched shape function for crack problems. Comput Methods Appl Mech Engrg 2017;322:541–62.
[207] Daphalapurkar NP, Lu H, Coker D, Komanduri R. Simulation of dynamic crack growth using the generalized interpolation material point (GIMP) method. Int J Fract 2007;143(1):79–102.
[208] Kakouris EG, Triantafyllou SP. Phase-field material point method for dynamic brittle fracture with isotropic and anisotropic surface energy. Comput Methods Appl Mech Engrg 2019;357:112503.
[209] Silling SA. Reformulation of elasticity theory for discontinuities and long-range forces. J Mech Phys Solids 2000;48(1):175–209.
[210] Silling SA, Epton M, Weckner O, Xu J, Askari E. Peridynamic states and constitutive modelling. J Elasticity 2007;88(2):151–84.
[211] Ren H, Zhuang X, Cai Y, Rabczuk T. Dual-horizon peridynamics. Internat J Numer Methods Engrg 2016;108(12):1451–76.
[212] Ren H, Zhuang X, Rabczuk T. Dual-horizon peridynamics: A stable solution to varying horizons. Comput Methods Appl Mech Engrg 2017;318:762–82.
[213] Rabczuk T, Ren H. A peridynamics formulation for quasi-static fracture and contact in rock. Eng Geol 2017;225:42–8.
[214] Zhou X, Wang Y, Qian Q. Numerical simulation of crack curving and branching in brittle materials under dynamic loads using the extended non-ordinary state-based peridynamics. Eur J Mech A Solids 2016;60:277–99.
[215] Dipasquale D, Zaccariotto M, Galvanetto U. Crack propagation with adaptive grid refinement in 2D peridynamics. Int J Fract 2014;190(1–2):1–22.
[216] Ha YD, Bobaru F. Studies of dynamic crack propagation and crack branching with peridynamics. Int J Fract 2010;162(1–2):229–44.
[217] Ha YD, Bobaru F. Characteristics of dynamic brittle fracture captured with peridynamics. Eng Fract Mech 2011;78(6):1156–68.
[218] Bobaru F, Zhang G. Why do cracks branch? A peridynamic investigation of dynamic brittle fracture. Int J Fract 2015;196(1–2):59–98.
[219] Butt SN, Meschke G. Peridynamic analysis of dynamic fracture: influence of peridynamic horizon, dimensionality and specimen size. Comput Mech 2021;67(6):1719–45.
[220] Bobaru F, Hu W. The meaning, selection, and use of the peridynamic horizon and its relation to crack branching in brittle materials. Int J Fract 2012;176(2):215–22.
[221] Chen Z, Ju JW, Su G, Huang X, Li S, Zhai L. Influence of micro-modulus functions on peridynamics simulation of crack propagation and branching in brittle materials. Eng Fract Mech 2019;216:106498.
[222] Cundall PA, Strack OD. A discrete numerical model for granular assemblies. Geotechnique 1979;29(1):47–65.
[223] Jing L, Stephansson O. Fundamentals of discrete element methods for rock engineering: theory and applications. Elsevier; 2007.
[224] Hedjazi L, Martin C, Guessasma S, Della Valle G, Dendievel R. Application of the discrete element method to crack propagation and crack branching in a vitreous dense biopolymer material. Int J Solids Struct 2012;49(13):1893–9.
[225] Lisjak A, Grasselli G. A review of discrete modelling techniques for fracturing processes in discontinuous rock masses. J Rock Mech Geotech Eng 2014;6(4):301–14.
[226] Leclerc W, Haddad H, Guessasma M. On the suitability of a discrete element method to simulate cracks initiation and propagation in heterogeneous media. Int J Solids Struct 2017;108:98–114.
[227] Hofmann H, Babadagli T, Zimmermann G. A grain based modelling study of fracture branching during compression tests in granites. Int J Rock Mech Min Sci 2015;77:152–62.
[228] Chung Y, Yang Z, Lin C. Modelling micro-crack initiation and propagation of crystal structures with microscopic defects under uni-axial tension by discrete element method. Powder Technol 2017;315:445–76.